# ANALYSIS AND DESIGN OF A SUBOPTIMAL, ADAPTIVE AUTOMATIC BRAKING SYSTEM

DOUGLAS W. HAROLD

# ANALYSIS AND DESIGN OF A SUBOPTIMAL, ADAPTIVE AUTOMATIC BRAKING SYSTEM

by

Douglas W. Harold, Jr.
Lieutenant, United States Navy
B.S., Rensselaer Polytechnic Institute, 1961



Submitted in partial fulfillment of the
requirements for the degree of

MASTER OF SCIENCE IN ELECTRICAL ENGINEERING

from the

NAVAL POSTGRADUATE SCHOOL
June 1968

ABSTRACT

A mathematical model of a vehicle being brought to rest in such a manner as to cause a skid is devised and simulated on an analog computer. This model includes the effects of the brake line pressure upon the braking of the vehicle and also the effects of the coefficients of friction between the tire and road surface and between the brake shoe and brake drum. Several controls to correct for the occurrence of a skid are simulated on the analog computer and a detailed analysis of the braking system under the influence of each control is performed. Lastly, a scheme for implementing the control which minimizes the stop time and the degree of skid is presented.

TABLE OF CONTENTS

LIST OF ILLUSTRATIONS

# 1. INTRODUCTION

Skidding of a vehicle due to an excessive application of brake force for the road conditions prevailing causes many thousands of accidents every year. Rapid and heavy application of brakes in a panic stop situation often causes wheel lock up and subsequent loss of control of the vehicle. This also occurs in wet or icy road conditions.

The minimum stopping distance possible for a vehicle is determined by the coefficient of friction between the tire and the road surface. When a vehicle is just on the verge of a skid the frictional force between the tire and road surface is at its greatest value, and consequently the deceleration of the vehicle is at a maximum, i.e., equal to $\mu_s g$, where $\mu_s$ is the coefficient of static friction between the tire and the road surface and g is the deceleration of gravity (see Appendix A for a proof of this statement).[7] When skidding occurs the tire slides along the road surface. This causes a reduction in the coefficient of friction and a corresponding reduction in the frictional force between the tire and road surface, thus decreasing the magnitude of the vehicular deceleration. The optimum braking situation would thus be attained if the vehicle could be kept just at the verge of a skid. If a skid could be detected exactly at the instant of occurrence and a compensating force were automatically applied to eliminate the skid before wheel lock up occurred, then nearly ideal braking conditions could be realized under all road conditions.

Attempts have been made previously to develop "anti-skid" devices, and some such devices are presently in use on certain aircraft and many trucks. Previous efforts in this direction include the Dunlop System of England, the Maxaret Unit, the Anti Skid Device, the Westinghouse Decelostat Controller, the Hydro-Aire Hytrol system, and the Anti-Skid Braking system of Russia's Tu - 104 Jet Liner.[1] These devices all work satisfactorily to a greater or lesser extent, but most have the drawback that operation depends upon the sensing of either a complete wheel lock up or the attainment of a pre-determined rate of wheel deceleration, at which time a bang-bang type of control is initiated. Additionally, many of these devices require expensive, heavy installations, rendering them largely unsuitable for economical installation and operation on commercial vehicles.

This thesis presents an analysis and evaluation of several electrically actuated alternate proposals designed to automatically compensate for an overbraking situation in order to minimize the degree of skidding and more nearly optimize the braking of a vehicle. A mathematical model for the system was developed and simulated on an analog computer, and three types of skid correcting controls were devised and tested. One form of control which linearly decreases the net force applied to the brake shoe until the skid is eliminated and then permits a linear increase of the net braking force until a skid once again occurs was tested. This is called the double ramp control. Two forms of bang-bang controls were also tested. Finally a triple ramp control which continually "samples" the road surface to determine the optimum brake force was devised and tested.

Complete data were obtained for each type of control and a detailed analysis was made of the behavior of the braking system under the influence of each control.

Lastly, a scheme for implementing the triple ramp control (which proved to be superior to any others devised) is advanced, although the physical system was not actually built.

## 2. DESCRIPTION OF THE PROBLEM

For the purposes of this paper, a skid will be defined as that condition which exists when the actual linear velocity of the frame of the vehicle in question is greater than the product of the angular velocity of the wheel and the radius of the wheel. In terms of the symbology used throughout this paper

$$e = V - R_1\omega, \tag{1}$$

$$e > 0 \quad \text{when } v > R_1\omega \tag{2}$$

and

$$e = 0 \quad \text{when } v = R_1\omega, \tag{3}$$

where v represents the linear velocity of the frame, $R_1$ represents the radius of the wheel and $\omega$ is the angular velocity of the wheel. The term e corresponds to an error signal, the magnitude of which is a measure of the degree of skidding present. The product $R_1\omega$ will be referred to as the velocity measured by the rotation of the wheel. When $e = 0$ there is no skidding and when $e > 0$ the vehicle is moving faster than a point on the rim of the wheel, i.e., the wheel is tending to lock up and a skid is occurring. The condition when $R_1\omega > V$ would occur when the wheels are spinning, as, for example, when trying to accelerate on an icy road.

A proposed means of sensing the linear velocity of the vehicular frame is to integrate the output from a linear accelerometer attached to the axle housing of the vehicle (to minimize effects of vehicle tilt during braking), and to compare the integrator output with the velocity measured by the rotation of the wheel. The initial condition

input to the integrator would be the velocity measured by the rotation of the wheel at the instant of application of the brake force.

When an error signal occurs, indicating skidding is present, an automatic corrective force ($F_c$) would be generated to reduce the total force F applied to the brakes. $F_{in}$ represents the force applied by the vehicle operator to the brakes and is considered constant for all subsequent analyses.

These concepts are illustrated in Fig. 1 where a block diagram of the proposed system is shown.[6]

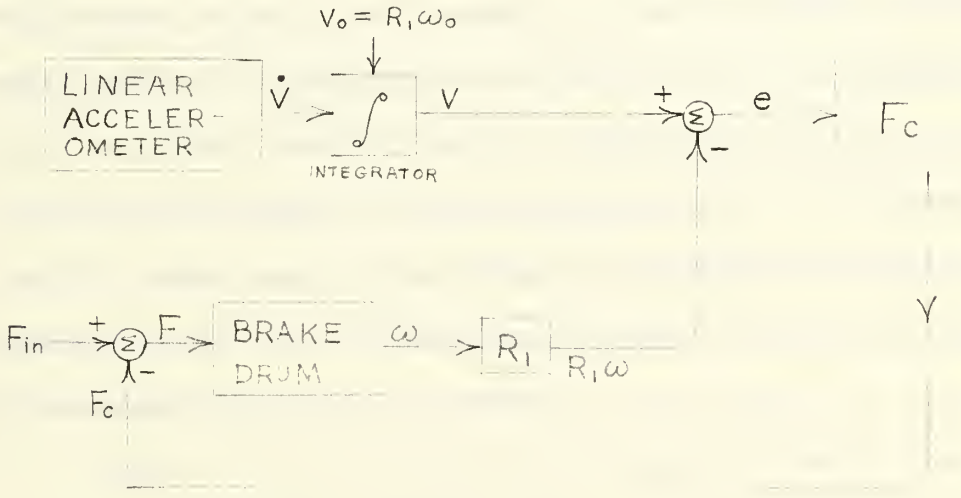


Fig. 1. Block diagram of the proposed braking system.

From elementary physics it is known that the coefficient of friction between two surfaces is dependent upon the relative velocity between the surfaces. A sketch of the behavior of the coefficient of friction as a function of the relative velocity between the two surfaces is shown in Fig. 2.[8]

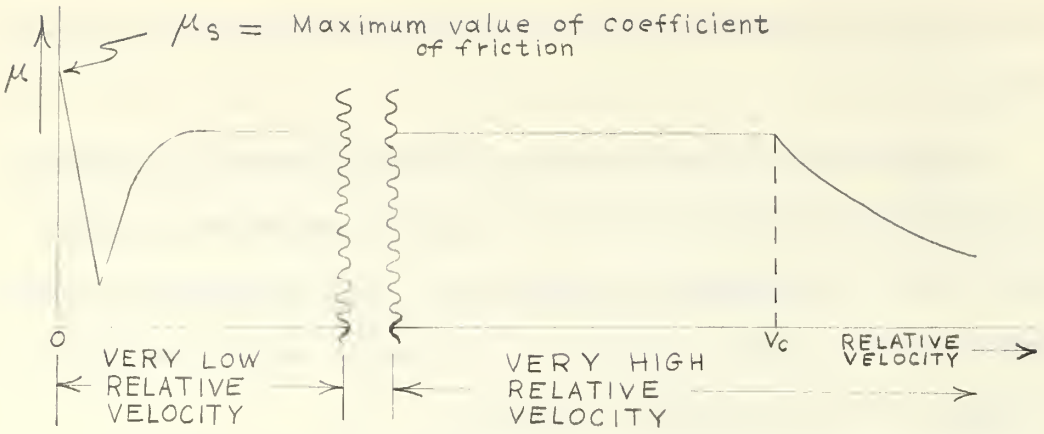


Fig. 2. Coefficient of friction as a function of relative velocity.

Just before relative motion begins, the coefficient of friction between two surfaces is at its maximum value. Prior to reaching this maximum value, the coefficient of friction is a variable that adjusts itself in such a manner so that the force tending to cause a relative motion is just compensated by the reactive force of friction (this is before any relative motion takes place). After sliding motion starts (as between a brake shoe and drum, or between a tire and road surface for a skidding situation) the coefficient of friction $\mu$ varies as shown.

A piecewise linear approximation to this behavior is shown in Fig. 3.

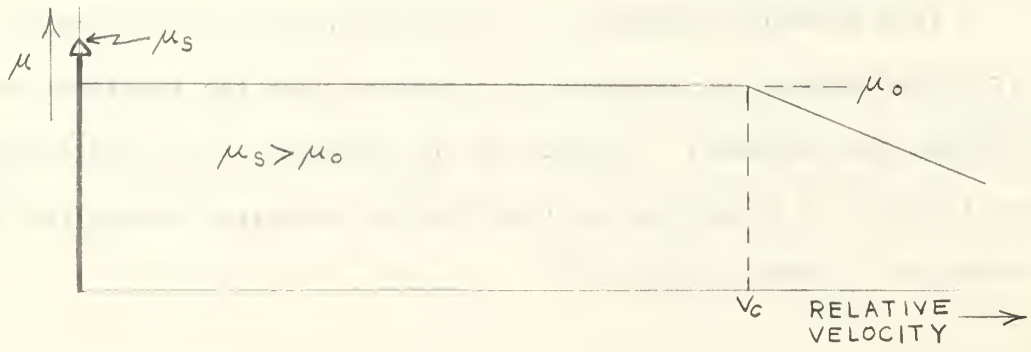


Fig. 3. Piecewise linear approximation to the behavior of the coefficient of friction.

The term $\mu_s$ corresponds to the coefficient of static friction which is a maximum just before relative motion begins, and which is always greater than the coefficient of kinetic or sliding friction.

The equation for this piecewise linear approximation is

$$\mu = \mu_o \text{ , for } \quad 0 < V < V_c \tag{4}$$

$$\mu = \mu_o - K_1'(V - V_c) \text{ , for } \quad V_c \leq V \leq \left(V_c + \frac{\mu_o}{K_1'}\right) . \tag{5}$$

The above relationship will be used to represent the coefficient of friction between the brake drum and brake shoe of the moving vehicle. The break point, $v_c$, for the coefficient of friction between the tire and the road surface will be assumed to be high enough so that for normal speeds the coefficient of kinetic friction is some constant $\mu_K$. As will be seen, this is not a restrictive assumption, since the purpose of the corrective forces to be applied is to minimize the degree of skid experienced. Thus the relative velocity between the tire and road surface would be small enough to warrant considering the coefficient of kinetic friction to be a constant.

Consider the idealized brake drum and shoe shown in Fig. 4.

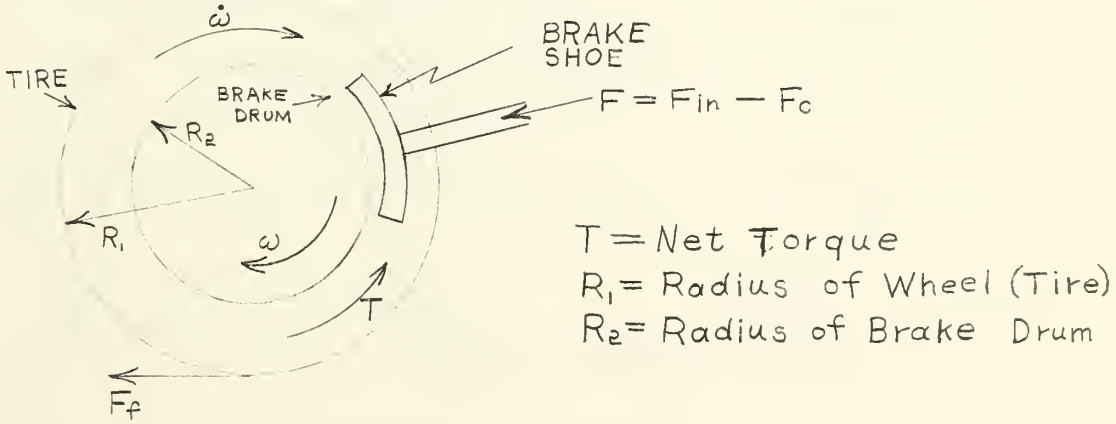


Fig. 4. Diagram of brake drum and shoe.

In Fig. 4 the wheel is assumed to be rotating in a clockwise direction with angular velocity $\omega$ and angular acceleration $\dot{\omega}$ with the positive sense as shown. F represents the total (net) force acting on the brake shoe, and is the difference between $F_{in}$ (applied by the brake pedal) and $F_c$ (the corrective force). $F_f$ is the force of friction, the value of which depends upon whether a skid is present. The equations describing this system are presented below.

$$F = F_{in} - F_c \tag{6}$$

$$\text{Net torque} = T = R_2 F\mu - R_1 F_f \tag{7}$$

$$F_f = \begin{cases} -m\dot{v} \text{ , for } e = 0 & (8) \\ \mu_K m g \text{ , for } e > 0 & (9) \end{cases}$$

where m = the weight of the vehicle acting through the axis of the wheel divided by the acceleration of gravity g (= 16 ft./sec.$^2$),

$$\mu = \begin{cases} \mu_o - K_1' R_2 (\omega - \omega_c) \text{ , for } \omega \geq \omega_c & (10) \\ \mu_o \text{ , for } \omega < \omega_c & (11) \end{cases}$$

i.e., $\mu$ is the coefficient of friction between the brake drum and brake shoe (Fig. 3). Also, $\mu_K$ is the coefficient of friction between the tire and the road when a skid is present.

Let $K_1' R_2 = K_1$ , so that Eq. (10) becomes

$$\mu = \begin{cases} \mu_o - K_1 (\omega - \omega_c) \text{ , for } \omega \geq \omega_c & (12) \\ \mu_o \text{ , for } \omega < \omega_c & (13) \end{cases}$$

and Eq. (7) becomes

$$T = R_2 F\mu - R_1 F_f = -J\dot{\omega} \tag{14}$$

where J = the moment of inertia of the wheel.

Consider the case where e = 0, i.e., skidding is absent, so

$$F_f = -m\dot{v} \leq \mu_s g \,, \tag{15}$$

with the equality holding when the system is just at the verge of a skid. The equation of motion, (14), becomes

$$-J\dot{\omega} = R_1 m\dot{v} + R_2 F\mu \,. \tag{16}$$

Since e = 0, then

$$\dot{v} = R_1 \dot{\omega} \,. \tag{17}$$

Substituting (17) into (16) yields

$$-J\dot{\omega} = R_1^2 m\dot{\omega} + R_2 F\mu \,. \tag{18}$$

Solving (18) for $\dot{\omega}$ yields

$$\dot{\omega} = \frac{-R_2 F\mu}{J + R_1^2 m} \,. \tag{19}$$

When e > 0, i.e., skidding is present, and

$$F_f = \mu_K mg \,, \text{ where } \mu_K < \mu_s \,, \tag{20}$$

then (14) becomes

$$-J_1\dot{\omega} = R_2 F\mu - R_1 \mu_K mg \,, \tag{21}$$

so

$$\dot{\omega} = \frac{R_1\mu_K mg}{J} - \frac{R_2 F\mu}{J} \,. \tag{22}$$

Note that for each of the relations for $\dot{\omega}$ the value of $\mu$ is a function of $\omega$. In the case where $\omega < \omega_c$, then $\mu = \mu_o$, and the equations above apply with $\mu$ replaced by $\mu_o$. When $\omega \geq \omega_c$, then

$$\mu = \mu_o - K_1(\omega - \omega_c) \,. \tag{23}$$

The complete set of equations is indicated below:

When e = 0, $\omega < \omega_c$ :

$$\dot{\omega} = \frac{-R_2 F}{J + R_1^2 m}\mu_o \,. \tag{24}$$

When $e > 0$, $\omega < \omega_c$ :

$$\dot{\omega} = \frac{R_1 \mu_K m g}{J} - \frac{R_2 F}{J} \mu_o \ . \tag{25}$$

When $e = 0$, $\omega \geq \omega_c$ :

$$\dot{\omega} = \frac{R_2 F K_1}{J + R_1^2 m} \omega - \frac{R_2 F K_2}{J + R_1^2 m} \ . \tag{26}$$

When $e > 0$, $\omega \geq \omega_c$ :

$$\dot{\omega} = \frac{R_2 F K_1}{J} \omega - \frac{R_2 F K_2}{J} + \frac{R_1 \mu_K m g}{J} \ . \tag{27}$$

In the last two relations,

$$K_2 \triangleq \mu_o + K_1 \omega_c \ .$$

The analog computer simulation of this system of equations is shown in Fig. 5. Note that Appendix B contains a brief description of the analog computer symbols used in this paper and an explanation of the logic elements used to control various portions of the simulation.[2,3,4,5]

To determine the equations governing the forward motion of the vehicle, recall that the maximum possible deceleration for a given coefficient of friction $\mu'$ between the tire and road surface is

$$-\ddot{x}_{max} = \mu' g \ , \tag{28}$$

where $\mu' = \mu_S$ or $\mu_K$ .

Thus, when $e = 0$, i.e., no skidding,

$$-\ddot{x} = -R_1 \dot{\omega} \leq \mu_S g \ , \tag{29}$$

where $\mu_S$ = the coefficient of static friction between the tire and the road surface. Also, before a skid occurs,

$$\dot{x} = R_1 \omega = V \ . \tag{30}$$

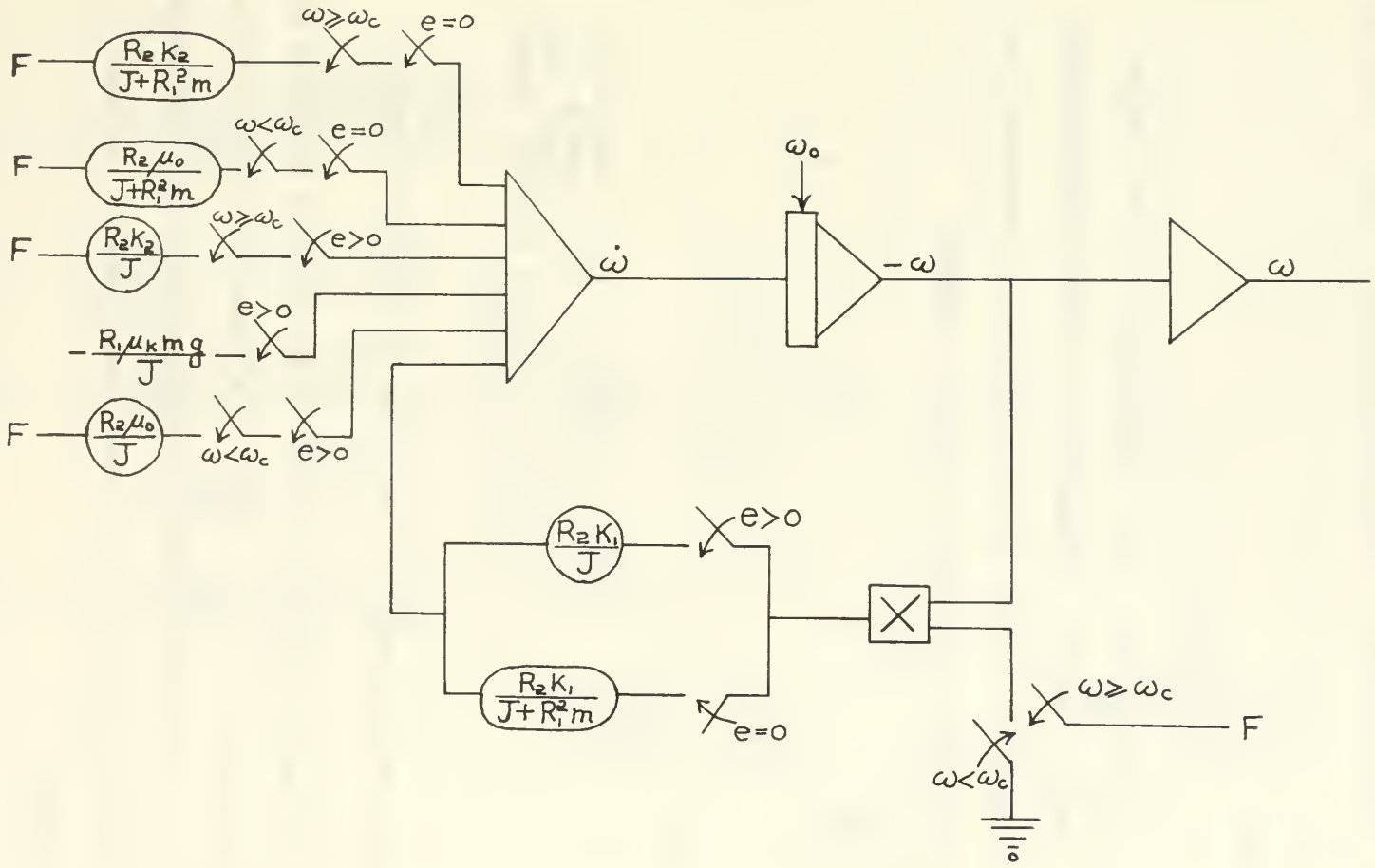


Fig. 5. Analog computer simulation of brake drum and shoe.

After a skid occurs,

$$\ddot{X} = -\mu_K g \quad ; \tag{31}$$

where $\mu_K$ = the coefficient of kinetic friction between the tire and road surface which is considered constant for this simulation, and $\mu_K < \mu_S$ .

Thus, when e > 0,

$$V = -\mu_K g t + V_o \quad ;$$

where $V_o$ is the velocity of the vehicle when the skid begins.

The analog computer implementation of these equations and ideas is presented in Fig. 6, which provides a simulation for V under conditions of skidding or skidless braking.

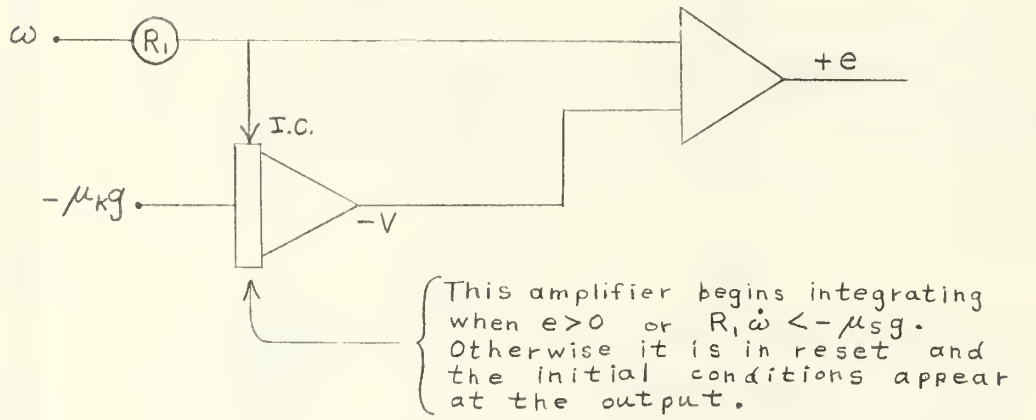


Fig. 6. Analog computer simulation of vehicular velocity.

The composite analog computer set up for both the brake drum and shoe and the vehicular velocity is shown in Fig. 7. This is intended to represent a conventional braking system in existence on present day vehicles and no corrective force is included in this diagram.

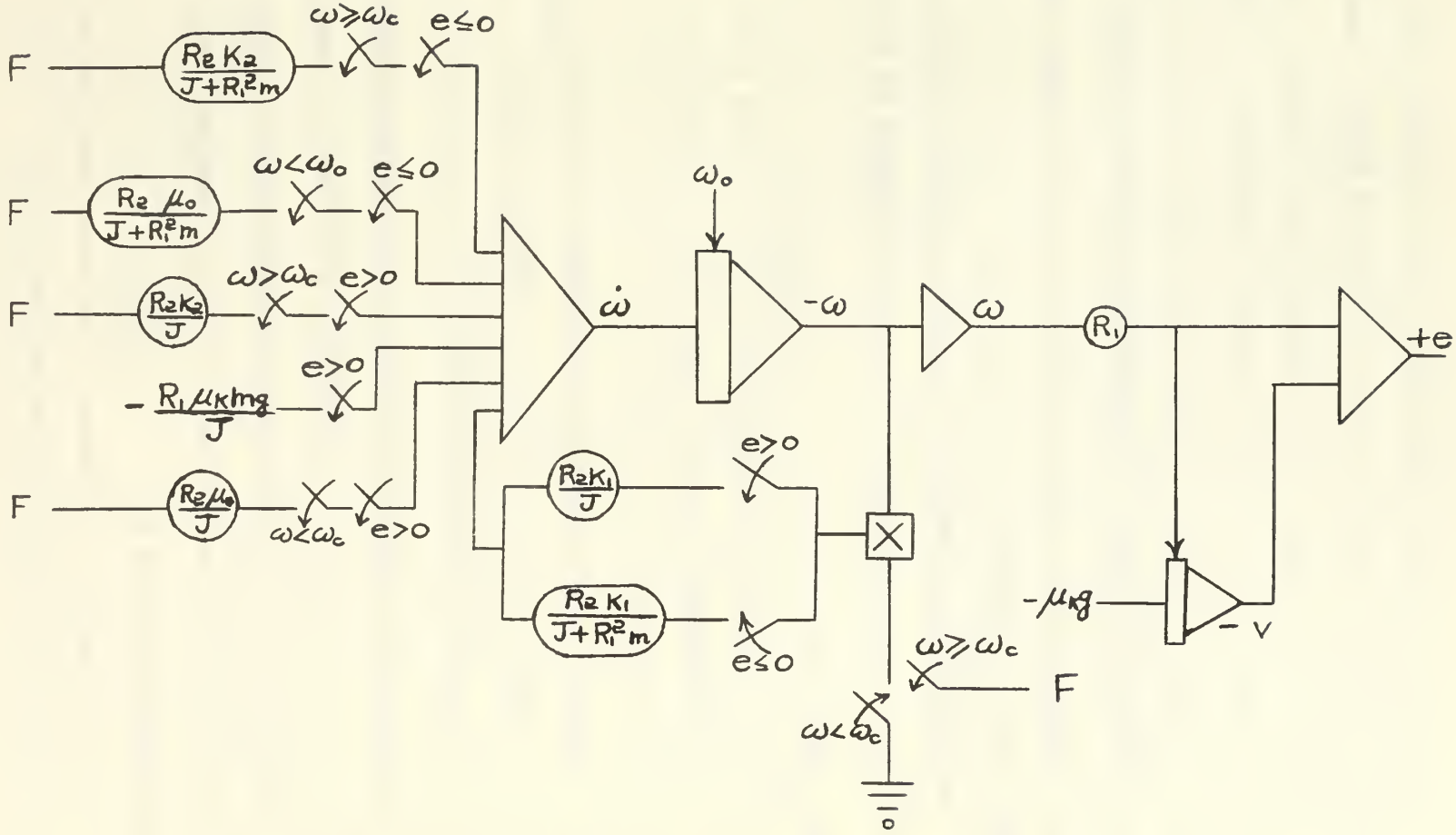


Fig. 7. Analog computer simulation of brake drum and shoe and vehicular velocity.

## 3. PROPOSED SKID CORRECTING CONTROLS

Any form of corrective control must be initiated by the occurrence of a skid, which in turn is indicated by the presence of a positive error signal. The purpose of the corrective control must be to lessen the net force F applied to the brake shoe when a skid is sensed. When the skid has ceased, the corrective force $F_c$ must decrease to permit a reapplication of the full braking force to the brake shoe. Thus the value of $F_c$ will depend upon whether a skid is present or not.

The first form of control to be tried is called a double ramp control, and a typical shape for the control is shown in Fig. 8.

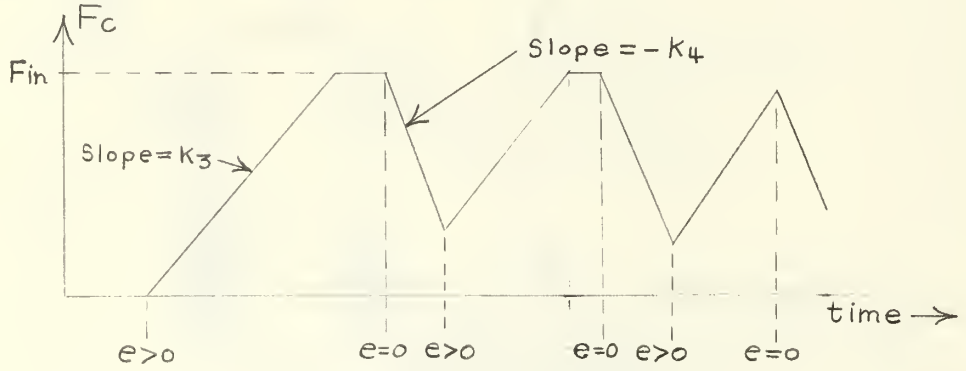


Fig. 8. Double ramp control.

An examination of Fig. 8 indicates that the maximum value attained by $F_c$ is $F_{in}$ (the force applied by the vehicle operator). Since $F = F_{in} - F_c$, and since there can never physically be a negative force on the brake shoe, $F_c \leq F_{in}$. The value of $K_3$ is not necessarily equal to $K_4$.

An analog computer simulation of the double ramp control is shown in Fig. 9.

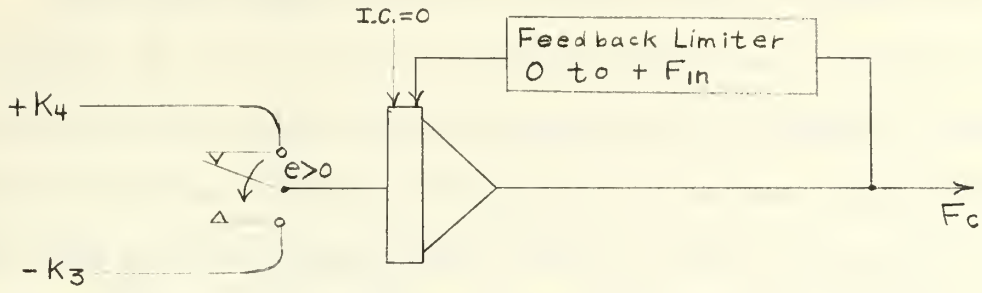


Fig. 9. Analog computer simulation of the double ramp control.

The integrator indicated in Fig. 9 may be in the compute mode for the entire problem simulation, due to the presence of the feedback limiter at the output of the integrator which prevents $F_c$ from ever going negative.

A bang-bang control was tried for the second form of corrective force. Since any physically realizable bang-bang control would have either a dead zone or a time delay, one control with a dead zone and one with a time delay were tried. The expression "dead zone" is meant to imply that there is some positive value of error voltage above which the corrective force is full on until the error is once again reduced to zero. The analog computer implementation of the bang-bang control with a dead zone is shown in Fig. 10, where $\alpha$ is the value of the dead zone voltage.

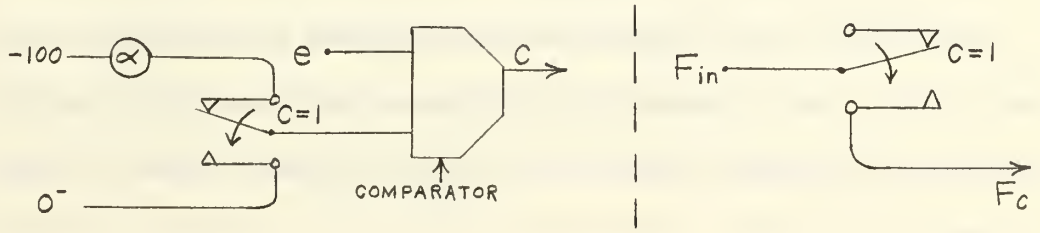


Fig. 10. Analog computer implementation of the bang-bang control with a dead zone.

The expression "time delay" as used here implies that the error exists for some time $T_1$ before corrective action is initiated. In order to simulate the time delay, a Wood fourth-order approximant [2] time lag circuit was set up to delay the error voltage by one second (real time delay), which in problem time corresponded to a delay time of 0.1 second. The analog computer diagram for the bang-bang control with a real time delay, with the potentiometer settings needed to produce a one second real time delay, is shown in Fig. 11.

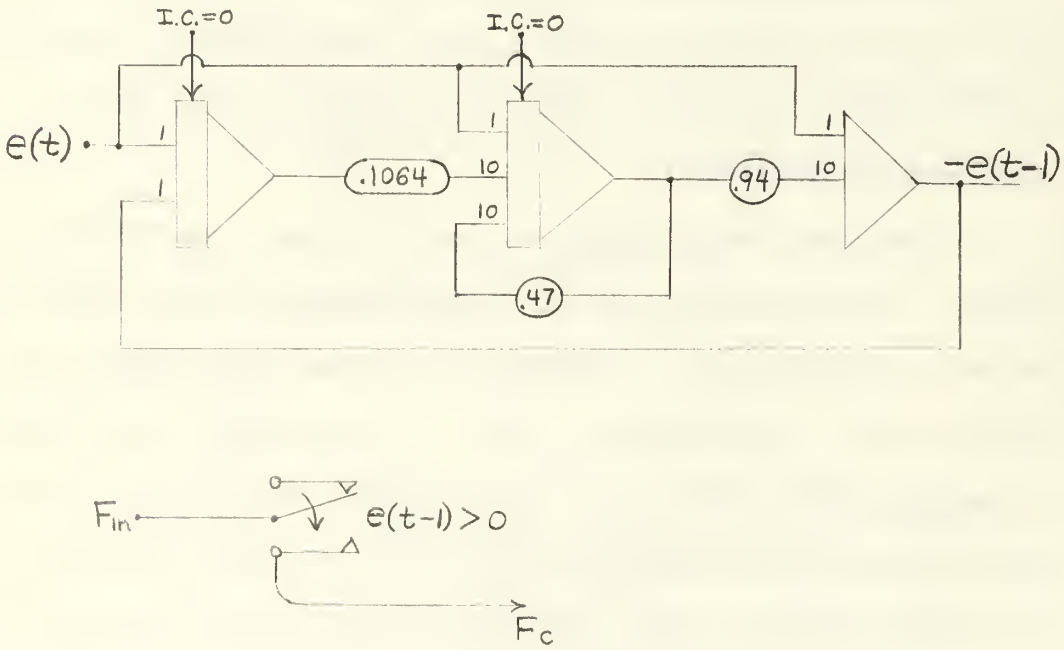


Fig. 11. Analog computer implementation of the bang-bang control with a real time delay.

The third form of control to be simulated is called the triple ramp control, and a typical plot of corrective force $F_c$ versus time plus the complementary plot of F (= $F_{in}$ - $F_c$) versus time is shown in Fig. 12.

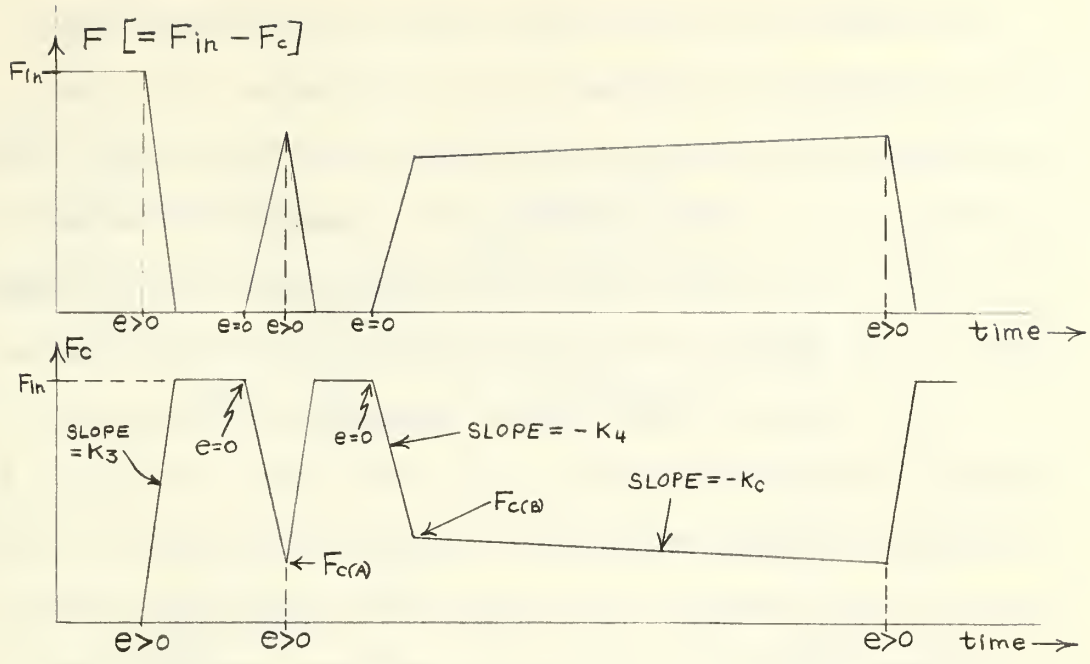


Fig. 12. Triple ramp control.

The triple ramp control is of the following form. $F_c = 0$ until a skid occurs. When a skid occurs, $e > 0$ and $F_c$ begins rising rapidly with a slope $K_3$ to a maximum value of $F_{in}$ or until $e = 0$. When $e = 0$, $F_c$ then begins decreasing with a slope equal to $- K_4$ until $e > 0$ once more. Up to this point the control is identical to the double ramp control. However, the second time that $e > 0$ a separate monitoring device with a "memory" (a Mylar capacitor, for example) holds the voltage at the value corresponding to the corrective force at which the skid occurred.

At the instant when $e > 0$ for the second time in Fig. 12, $F_c$ would once again increase rapidly with slope $K_3$ until $e = 0$. Then $F_c$ would again begin decreasing with slope $- K_4$ until it is just above the corrective force at which skidding occurred previously. Then $F_c$ would be allowed to decrease more slowly with a slope $- K_c$ (thus permitting a gradual increase in F until a skid once again occurs). The cycle then repeats itself.

The design of this particular type of control was motivated by the considerations expressed in the Introduction, i.e., that the optimum braking situation would be realized if the vehicle could be kept just at the verge of a skid. The storage of the value of $F_c$ at which a skid occurs endows the control with a form of "intelligence" which permits the net force applied to the brake drum to be just less than the optimum force. The gradual increase in F permitted by the third portion of the control (with a slope of $- K_c$) is necessary to permit the control to adapt to improving (i.e., less slippery) road conditions. The first cycle of the control, where $F_c$ increases rapidly with a slope of $K_3$ and then decreases with a slope of $- K_4$ until the skid occurs once again, is necessary to permit the control to "test" the road surface for the net force required to just cause a skid. The analog computer implementation of this control is shown in Fig. 13.

Integrator No. 1 provides the ramp with a slope of $K_3$, $- K_4$, or $- K_c$ as appropriate. This integrator is in the compute mode for the entire simulation time and $F_c$ is kept from going negative by the lower bound of the feedback limiter. The upper bound on the limiter, and consequently on $F_c$, is determined by $F_{in}$. Potentiometer No. 1, labeled C.R./10, determines the value of $F_c$ at which the slope changes from $- K_4$ to $- K_c$; the ratio of $F_{c(B)}/F_{c(A)}$ (see Fig. 12) is termed the Correction Ratio (C.R.). It is this ratio which determines the setting of potentiometer No. 1. When integrator No. 2 is in the track (reset) mode switch No. 1 is closed ($\overline{FF} = 1$) and we desire the slope of $F_c$ to be either $K_3$ or $- K_4$ (but not $- K_c$), since this is the time period between the first and second occurrences of the positive error signal. Thus to positively prevent relay No. 1

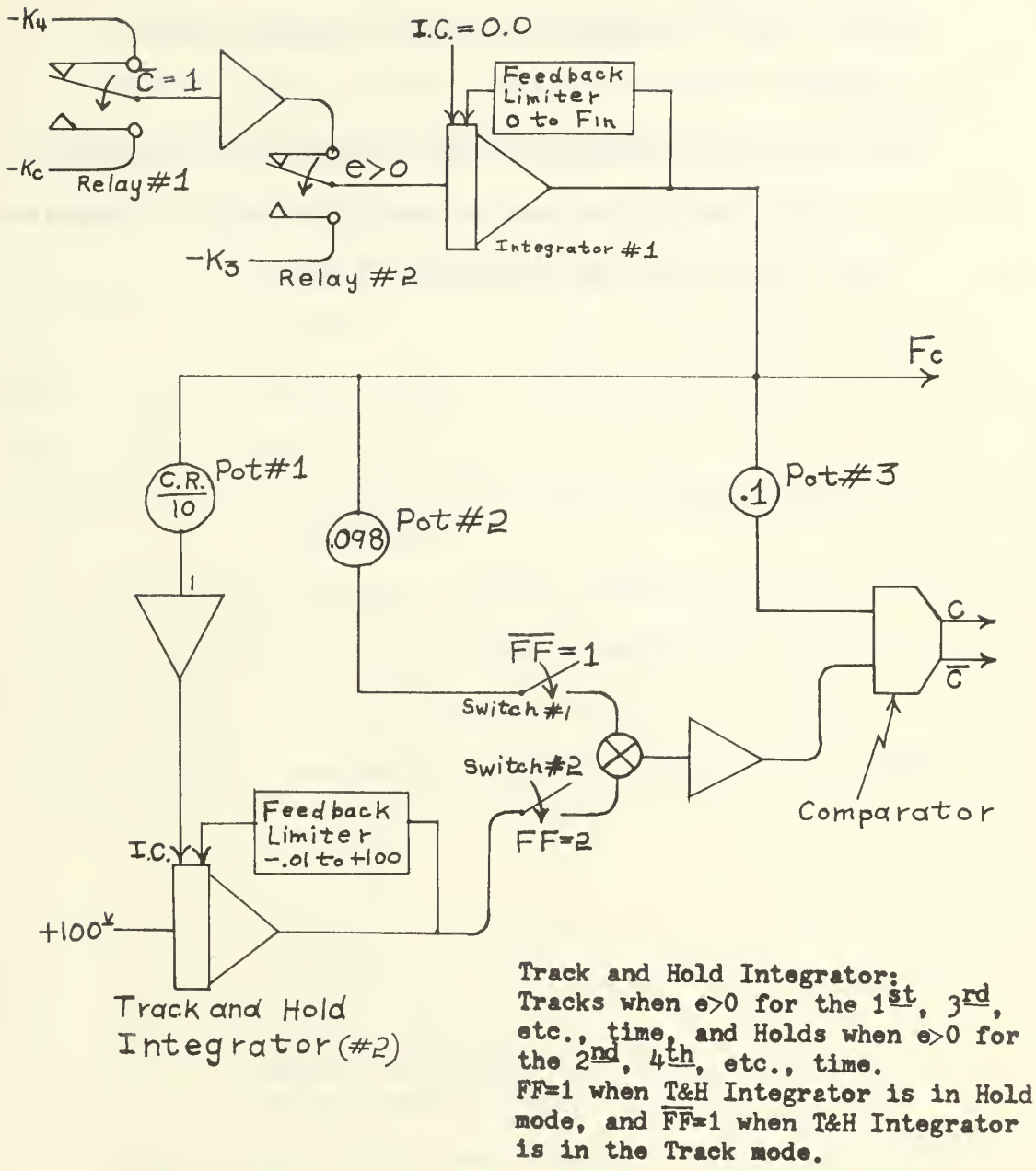


**Fig. 13. Analog computer implementation of the triple ramp control.**

from throwing during this phase of the cycle potentiometer No. 2 is set lower than potentiometer No. 3 to insure that C = 1 and $\overline{C}$ = 0, where 1 and 0 correspond to a logical true and false, respectively.

The flip flop (the output of which is denoted by FF and $\overline{FF}$) is an R - S flip flop, and is used to control the mode of integrator No. 2 as well as the state of switches No. 1 and 2.

## 4. THE UNCONTROLLED SITUATION

The analog computer simulation of the uncorrected braking of the vehicle (shown in Fig. 7) was set up on the COMCOR Ci 5000 Analog Computer, using the following arbitrary parameters:

$K_1 = 0.01$

$\omega_c = 60$ rad./sec.

$\mu_o = 0.8$

Thus $\mu = 0.8 - 0.01\ (\omega - 60),\ \omega \geq \omega_c$

and $\mu = 0.8,\ \omega < \omega_c,$

where $\mu$ = coefficient of friction between the brake drum and shoe.

$\mu_s = 0.75 \Longrightarrow$ static friction between tire and road surface.

$\mu_K = 0.5 \Longrightarrow$ kinetic friction between tire and road surface.

$V_o = 75$ ft./sec. = initial vehicular velocity.

$\omega_o = 75$ rad/sec. $\Longrightarrow$ initial rotational velocity of the wheel.

$R_1 = 1$ ft.

$R_2 = .6$ ft.

$J = 25$ ft. lb. sec.$^2$

$M = 93.75$ slugs

(Weight = mg = 2000 lbs. = weight of vehicle acting through axis of wheel).

A 7000 lb. input force (corresponding to $F_{in}$) was simulated as a 70 volt step input occurring at time = 0 sec.

Six different variables were plotted for each run on a Brush Instruments Mark 200 (6 channel) Recorder. They were

$\dot{\omega} \Longrightarrow$ the angular acceleration of the wheel, in rad/sec.$^2$

$\omega \Longrightarrow$ the angular velocity of the wheel, in rad/sec.

$V \Longrightarrow$ the actual linear velocity of the vehicle, in ft/sec.

$F \Longrightarrow$ the net force applied to the brake shoe ($= F_{in} - F_c$), in lbs.

$e \Longrightarrow$ the error signal ($= v - R_1\omega$), in ft/sec.

$F_c \Longrightarrow$ the corrective force, in lbs.

The uncorrected system response of the vehicle, i.e., the response obtained when no corrective force is applied, is shown in Fig. 14. From examination of the uncorrected system plot it is seen that the wheel locks in 0.96 sec. and skidding occurs 0.16 sec. after application of the braking force. The skid is present until the vehicle comes to rest 4.64 sec. after the force is initially applied.

Measuring the slope of the velocity output plot gives an average deceleration of 16 ft/sec.$^2$ (excluding the first 0.1 sec. of the problem, where skidding does not occur). This is expected, since with $\mu_K = 0.5$ the deceleration during a skid is 16 ft/sec.$^2$ ($= 0.5 \times 32$ ft/sec.$^2$).

To completely understand the shapes of the various plots displayed in Fig. 14, recall that the coefficient of friction between the brake drum and brake shoe is of the general shape indicated in Fig. 3, with a break point at $\omega_c = 60$ rad/sec. The initial rotational velocity of the wheel was $\omega_o = 75$ rad/sec., and thus at the time of simulated application of the brakes the coefficient of friction $\mu$ between the brake drum is

$$\mu = 0.8 - 0.01\ (75 - 60) = 0.65.$$

The value of $\mu$ will increase as the relative velocity between the brake shoe and brake drum decreases, until it has attained a maximum value of 0.8. After the problem begins there is a time lapse

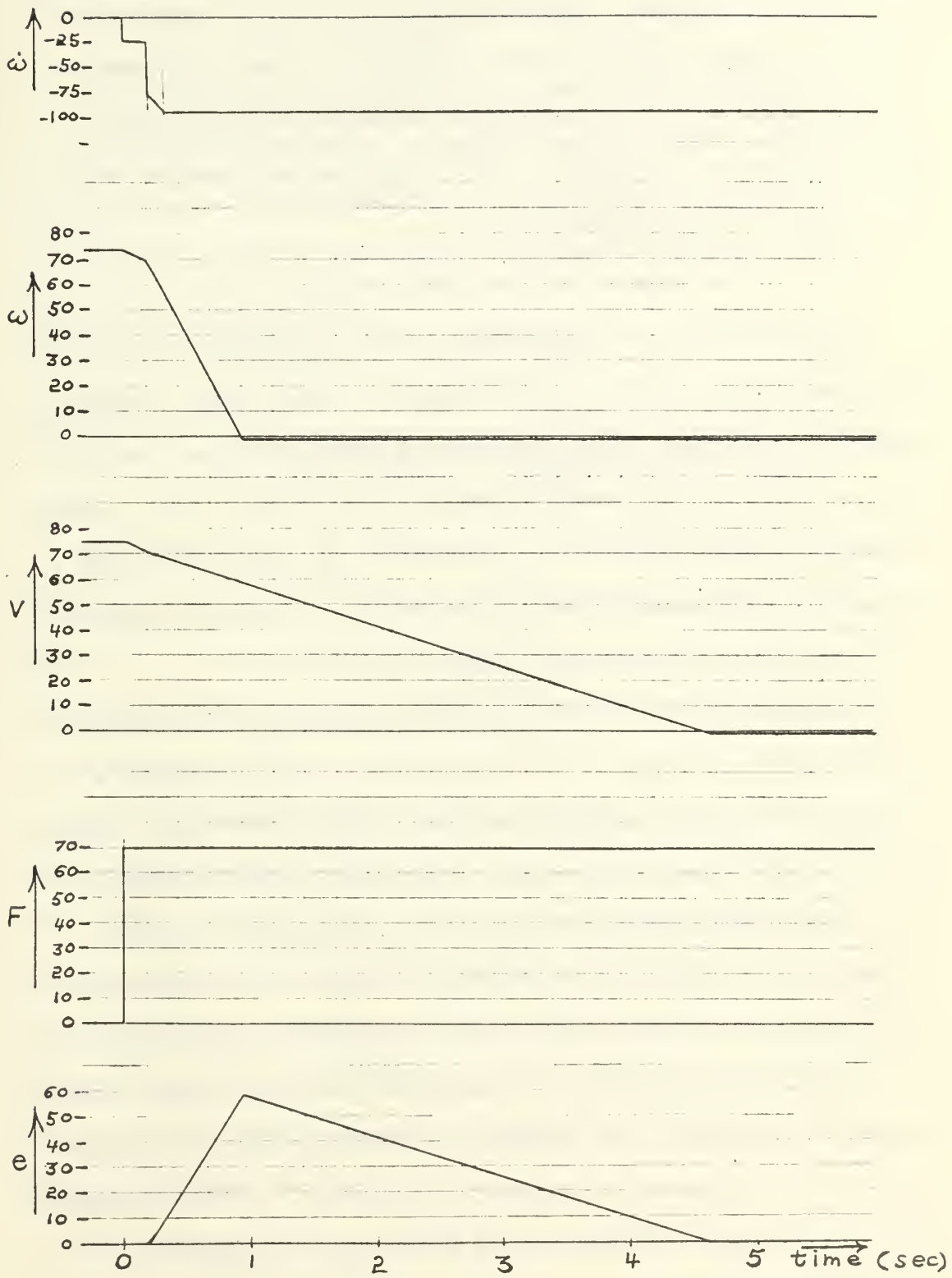


Fig. 14. Uncorrected braking situation.

of 0.16 sec. before skidding starts. During this initial 0.16 sec. $\mu$ is increasing since the vehicle is slowing down. However, $\mu$ is sufficiently small during this time interval so that the net torque T ($= R_2F\mu - R_1F_f$) acting on the wheel is not sufficient to cause a skid. When the velocity has decreased to 70 miles/hr., and $\omega$ is down to 70 rad/sec. (since a skid has not occurred yet), the value for $\mu$ has increased to

$$\mu = 0.8 - 0.01\ (70 - 60) = 0.7.$$

This value for $\mu$ is sufficiently large to cause the net torque to be just equal to that value necessary to cause a skid. At the instant a skid occurs the coefficient of friction between the tire and road surface drops abruptly from $\mu_s = 0.75$ to $\mu_K = 0.5$. $F_f$ also decreases abruptly due to the occurrence of the skid and the net torque increases rapidly, causing the wheel to decelerate rapidly and lock after 0.96 sec. total elapsed time.

Note that the plot for the radial acceleration of the wheel $\dot{\omega}$ indicates that at time = $0^+$ the acceleration drops sharply to a negative value (- 23 rad/sec.$^2$) and then slowly becomes more negative until the time when a skid occurs. During this time the wheel is still slowing down gradually, and the deceleration (or negative acceleration) is increasing slowly as the value of $\mu$ (between the brake shoe and brake drum) increases. At the point when the value of $\dot{\omega}$ becomes just less than - 24 rad/sec.$^2$, the skid occurs, and $\dot{\omega}$ abruptly becomes much more negative (- 76 rad/sec.$^2$) and decreases rapidly until it reaches a constant - 94 rad/sec.$^2$ The significant factor to be noted here is that the skid occurs just when $\dot{\omega} =$ - 24 rad/sec.$^2$. This corresponds to a value of $\dot{V}$ = - 24 ft/sec.$^2$ (since $R_1$ = 1 ft., and a skid has not occurred yet). This is in

agreement with the previous statement that the maximum deceleration possible without a skid occurring is

$$\mu_s g = -0.75 \times 32 \text{ ft/sec.}^2 = -24 \text{ ft/sec.}^2.$$

The leveling off of the $\dot{\omega}$ plot at - 94 rad/sec.$^2$ occurs at the time when the rotational velocity $\omega$ crosses the 60 rad/sec. mark which is the value established for the critical value of rotational velocity $\omega_c$, below which $\mu$ becomes a constant = 0.8. Since $\mu$ is constant and

$$F_f = \mu_K mg$$

then the net torque T is

$$T = R_2 F\mu - R_1 \mu_K mg = \text{a constant, and } \dot{\omega} \text{ is thus a constant.}$$

The magnitude of the error rises to a maximum value and then decreases to zero when the vehicle has completely stopped. This behavior is expected when it is noted that the error is merely the difference between the linear velocity and the rotational velocity of the wheel.

One other comment concerning the response of the uncorrected system is appropriate. Inspection of the vehicular velocity v plot reveals that a steeper slope is present on the plot prior to the beginning of a skid. After the skid begins the slope becomes less steep and remains constant until the vehicle comes to rest. The deceleration of the vehicle is thus greater before the skid begins than it is after skidding occurs, which is in accordance with the expected results.

The important fact to notice is that during a large part of the path the vehicle is in what would be an uncontrolled skid, as

shown by the large magnitude of the error. This uncontrolled skid is a matter of as much concern as the lengthened time to stop the vehicle. This lengthened time is caused by the effect of the smaller coefficient of friction which acts between the tire and the road surface when skidding is occurring. The optimum time of stopping, assuming braking takes place just at the verge of skidding, is

$$t \text{ optimum} = \frac{75 \text{ ft/sec.}}{24 \text{ ft/sec.}^2} = 3.13 \text{ sec.},$$

where 24 ft/sec.$^2$ is the maximum possible deceleration using the values assumed for this simulation.

## 5. THE DOUBLE RAMP CONTROL

The various proposed controls described in Section 3 were implemented in an attempt to obtain a more nearly optimal braking situation. The first of these corrective forces was the double ramp control shown in Fig. 8. A total of 21 separate runs were made with this form of control. $K_4$ was initially held constant at 40000 lbs/sec., and $K_3$ was varied from 5000 lbs/sec. up to 60000 lbs/sec. Then $K_3$ was held constant at 60000 lbs/sec. and $K_4$ varied from 5000 lbs/sec. to 50000 lbs/sec. Finally, two runs were made with $K_3$ and $K_4$ set at 80000 lbs/sec. and at 100000 lbs/sec. Representative samples of the behavior to be expected from this form of control are shown in Fig. 15 where $K_3$ = 60000 lbs/sec. and $K_4$ = 35000 lbs/sec., and in Fig. 16 where $K_3$ = 100000 lbs/sec. and $K_4$ = 100000 lbs/sec.

An examination of Fig. 15 indicates that for the specific values of $K_3$ and $K_4$ chosen (i.e., 60000 lbs/sec. and 35000 lbs/sec. respectively) the stop time has been increased to 5.47 sec., whereas the stop time under controlled conditions was only 4.64 sec. However, the total time during which a skid is occurring has been reduced to 2.08 sec. and the magnitude of the skid has been reduced to approximately 2 ft/sec. during the entire braking cycle. These figures are contrasted to a total skid time of 4.47 sec. and a maximum magnitude of skid of 68 ft/sec. for the uncorrected situation.

When the brakes are initially applied at time = 0 sec. there is a time lapse of 0.16 sec. before a skid occurs. This is exactly the same situation that occurs in the uncorrected braking and is accounted for by the same reasoning. After 0.16 sec., a skid commences. This

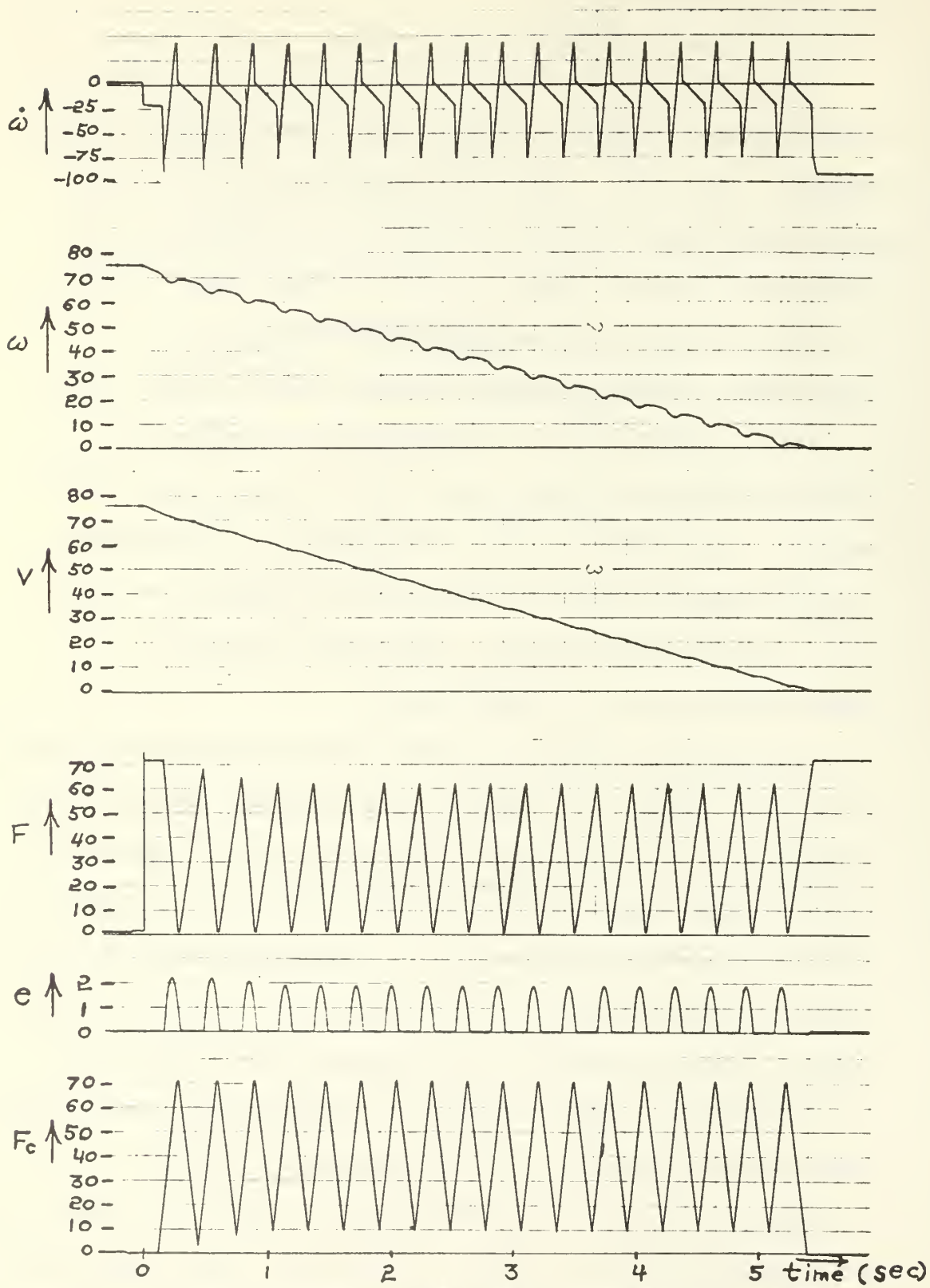


Fig. 15. Double ramp control response, $K_3$ = 60000 lbs/sec.,

$K_4$ = 35000 lbs/sec.

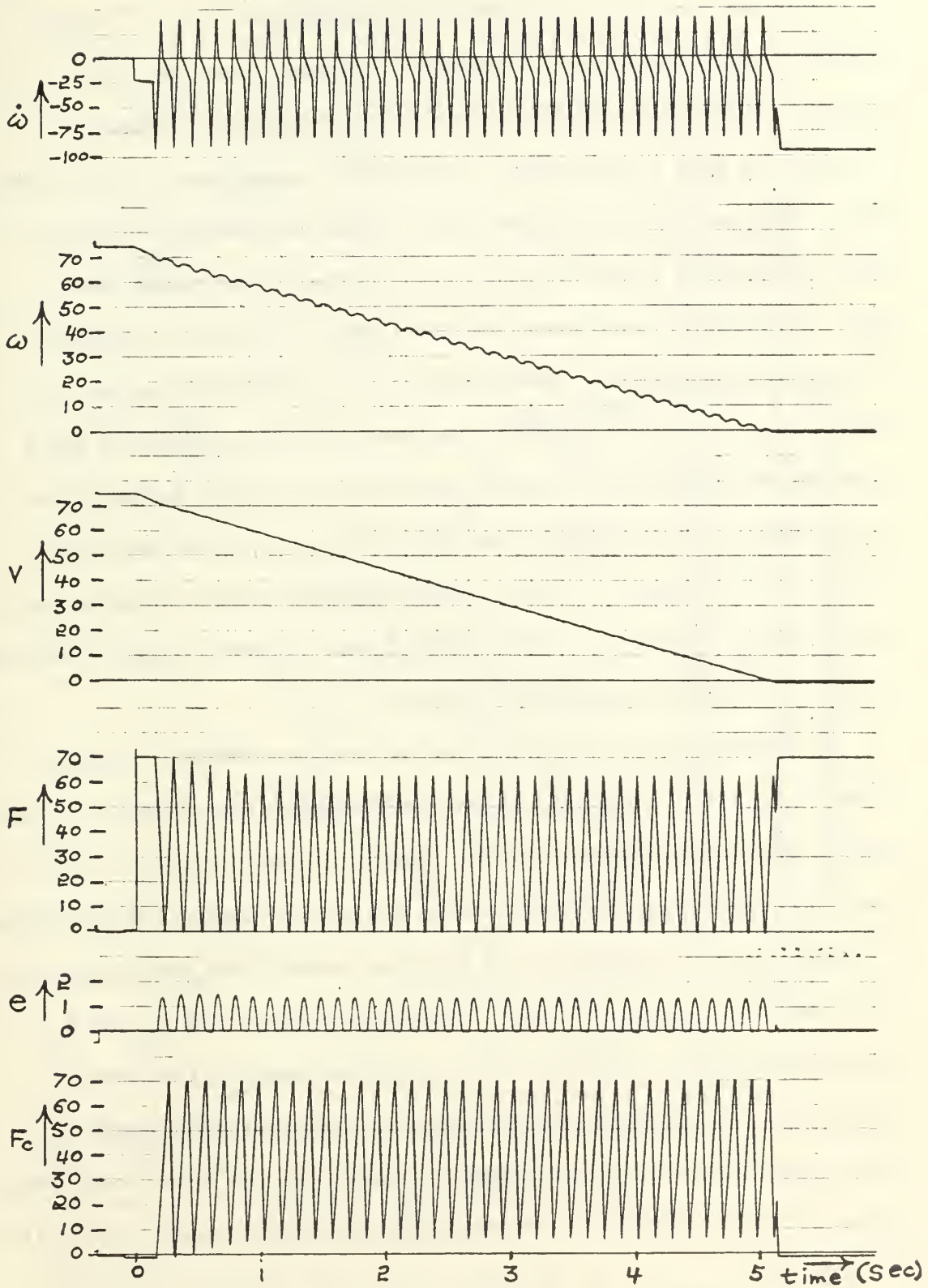


Fig. 16. Double ramp control response, $K_3$ = 100000 lbs/sec., $K_4$ = 100000 lbs/sec.

is indicated in Fig. 15 by the positive going error signal and also by the abrupt drop of the $\dot{\omega}$ plot from - 24 rad/sec.$^2$ to approximately - 78 rad/sec.$^2$. Recall that when skidding occurs the net torque acting to slow the wheel is suddenly increased, thus the wheel starts to slow down rapidly, as seen from inspection of the $\omega$ versus time plot at the time of the initial occurrence of the first skid. However, the corrective force immediately begins acting to decrease the net force F (= $F_{in}$ - $F_c$) acting on the brake shoe, which consequently decreases the net torque T (= $R_2F\mu$ - $R_1\mu_K mg$), and the wheel begins to speed up to "catch up" with the velocity of the vehicle. This accounts for the sudden positive slope of the $\dot{\omega}$ plot almost immediately after an error signal occurs, and also for the upswing on the $\omega$ versus time plot after the initial drop of $\omega$ with each occurrence of a skid. The corrective force increases until it equals $F_{in}$ and/or e = 0 once more, at which time it begins decreasing towards zero until a skid occurs again.

An expanded plot of $\omega$ and v versus time for two skid cycles is shown in Fig. 17. To obtain this plot the equations of motion of the system were solved numerically by slide rule with the value of $K_3$ = 5000 lbs/sec. and $K_4$ = 8000 lbs/sec.[9] Also, the simplifying assumption was made that the coefficient of friction between the brake drum and brake shoe was constant at 0.8. While these values for $K_3$ and $K_4$ and the simplifying assumption for $\mu$ were not used in the analog computer runs, the shape of the curves is similar to the shape of those obtained on the analog computer simulation. A brief explanation of Fig. 17 will facilitate understanding the curves shown in Fig. 15 and Fig. 16.

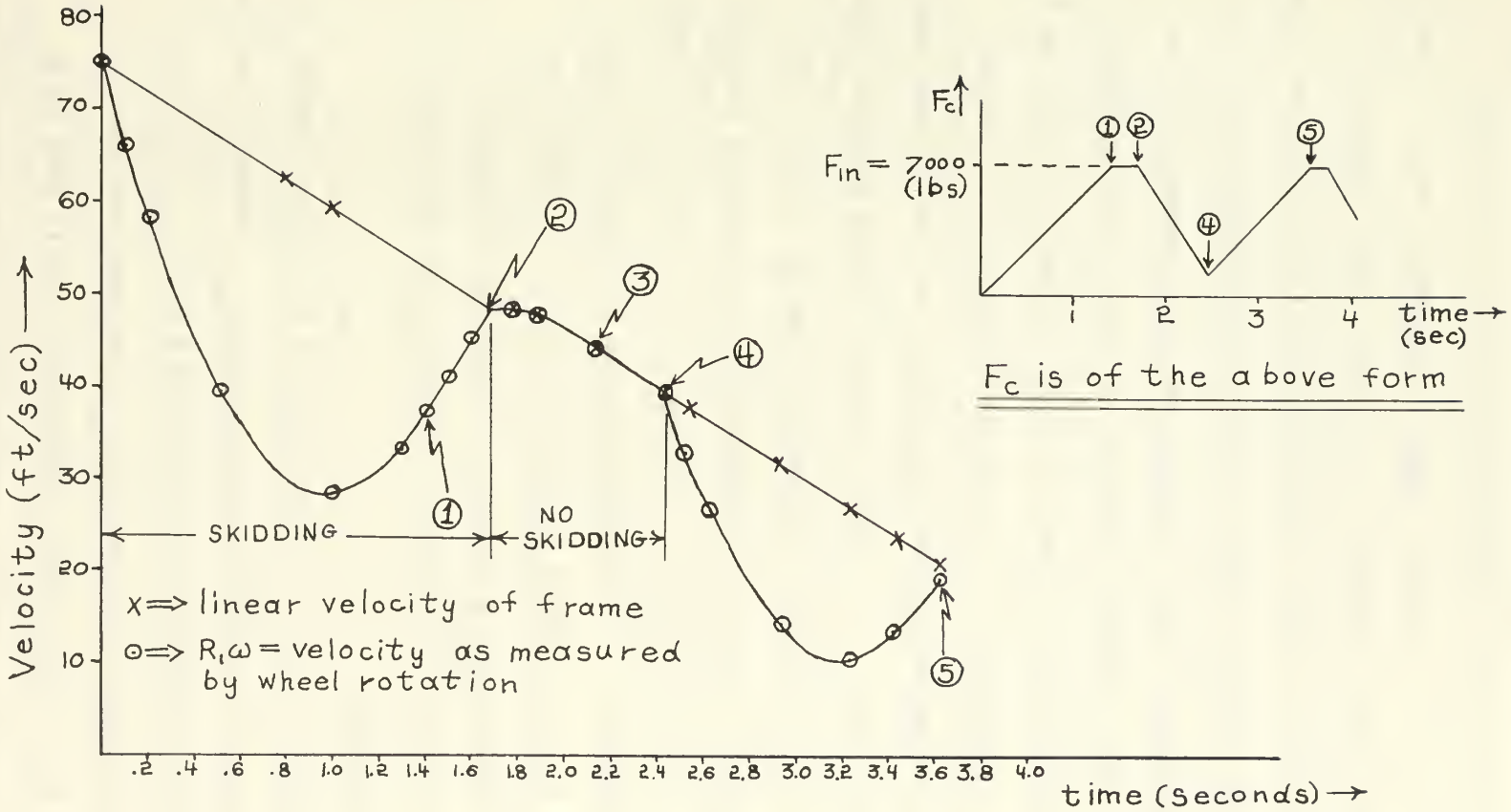


**Fig. 17. Expanded plot of wheel velocity and vehicular velocity versus time for the double ramp control.**

Referring to Fig. 17, note that a skid begins at time = $0^+$ sec. This is due to the simplifying assumption of a constant $\mu = 0.8$ over the entire velocity range of interest, and in no way affects the qualitative aspects of the curve shown. The value of $\omega$ (or $R_1\omega$ as plotted in Fig. 17) decreases initially and then rises to intersect the velocity V plot (which is decreasing linearly as the vehicle skids). For time less than the point marked (1), the slope of the $\dot{\omega}$ curve would be positive, as can be seen by mental differentiation of the $R_1\omega$ curve. This is in agreement with the $\dot{\omega}$ curve of Fig. 15 and Fig. 16. At the point marked (1), however, the $R_1\omega$ curve now begins increasing linearly, and the $\dot{\omega}$ curve would have a constant value, i.e., would level off at some positive value corresponding to the slope of the segment from (1) to (2). This leveling off of the $\dot{\omega}$ plot is observed also in the analog computer results of Fig. 15 and Fig. 16. The time period when the leveling off occurs corresponds to the region between (1) and (2) of the inset plot of $F_c$, i.e., where $F_c$ has attained its maximum value and the net torque is now a constant. Since the net torque is constant, the value of $\dot{\omega}$ is also a constant, until the skid is completely eliminated.

At point (2) the skid is eliminated and $F_c$ begins dropping to permit reapplication of the full brake force $F_{in}$. However, the net force F increases gradually from zero with a slope $K_4$, and for a significant time after the elimination of the skid the velocity is decreasing at an unacceptably slow rate. This is seen by an inspection of the region of the curve of Fig. 17 from point (2) to (4). At point (3) the deceleration has finally increased to that

value of deceleration experienced in a skid, i.e., - 16 ft/sec.$^2$, and at point ④ it is sufficiently great to cause a skid to occur once more. The process then repeats itself.

The rather detailed qualitative analysis undertaken above serves to point up the major defects inherent in the double ramp form of control. If the parameters $K_3$ and $K_4$ are chosen so as to maximize the time when a skid is not occurring, e.g., to maximize the time from point ② to point ④ of Fig. 17, then the time from point ② to ③ will also be maximized. From ② to ③ the velocity is decreasing at less than the optimum rate, and even at less than the deceleration experienced when in a skid. Thus it would seem that by minimizing the skid time with the double ramp control, we are inadvertently maximizing the actual time to stop. This conclusion is borne out by the results of Fig. 18 and Fig. 19, where the skid times and stop times for the various values of $K_3$ and $K_4$ simulated on the analog computer are plotted.

Figure 20 is a plot of the magnitude of the skid observed versus $K_3$, with $K_4$ fixed at 40000 lb/sec. The magnitude of the skid after it has obtained a constant value is the value that is plotted here. It is seen that the magnitude of the skid is very dependent upon the value of $K_3$, which is an expected result since the larger the value of $K_3$, the more rapidly is the skid corrected. This also accounts for the decrease in the skid time with increasing $K_3$ observed in Fig. 18. Experimental results indicated that the magnitude of the skid is unaffected by the value of $K_4$, which is natural since the downward going portion of the double ramp control is only acting when no skid is present. The stop time is increased, however, with increasing $K_3$

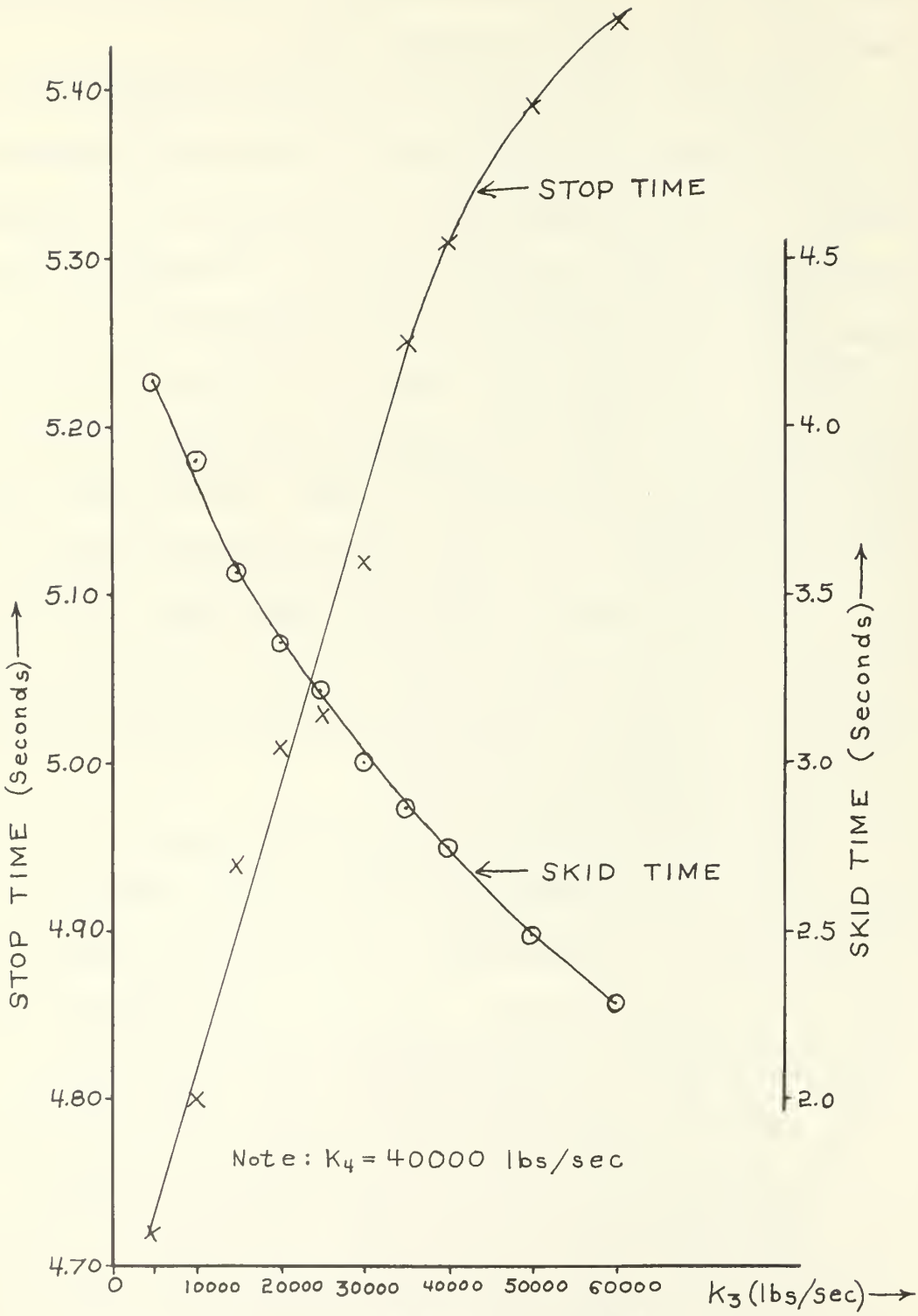


**Fig. 18. Stop time and skid time versus $K_3$ for the double ramp control.**

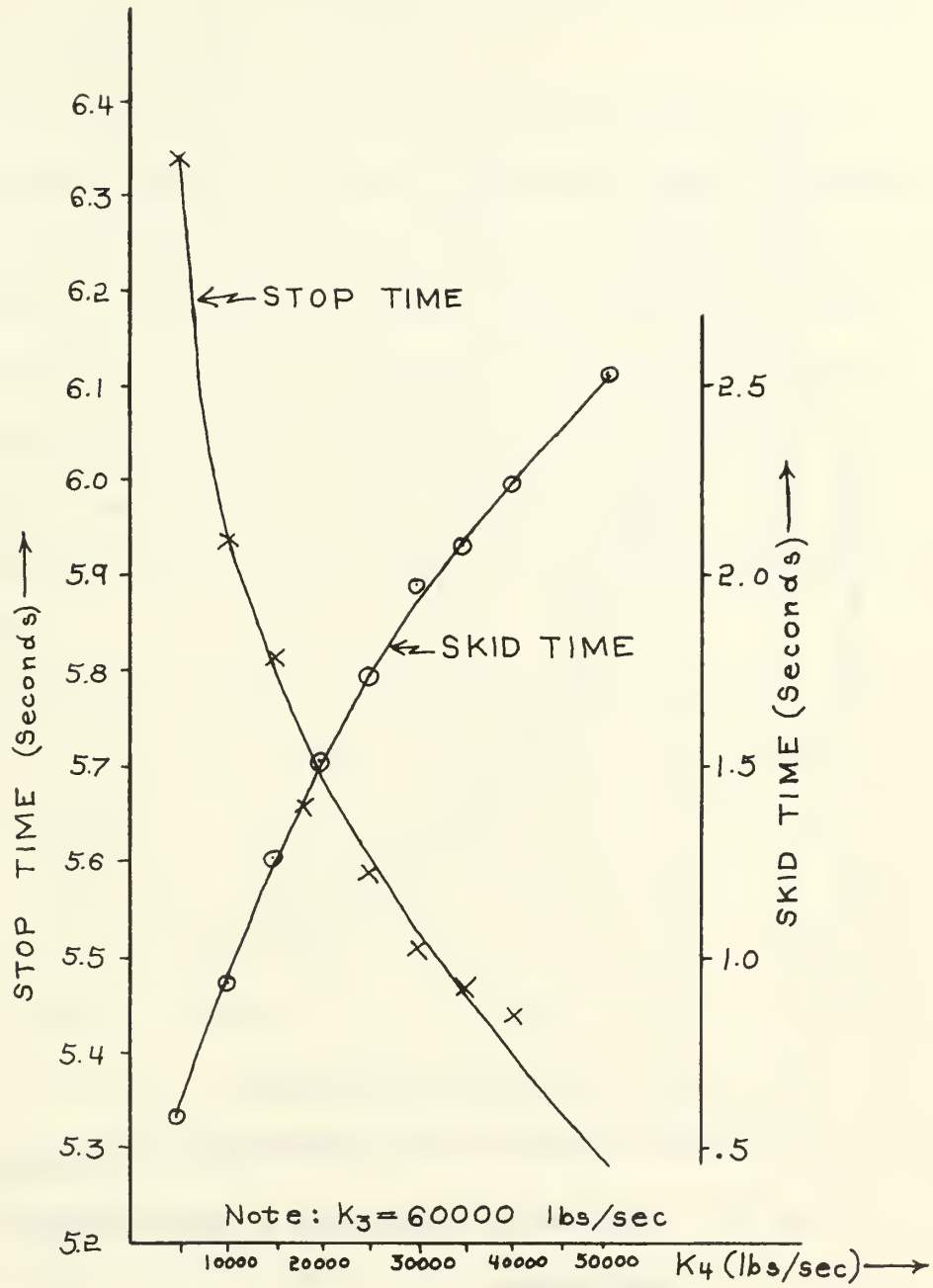


**Fig. 19. Stop time and skid time versus $K_4$ for the double ramp control.**

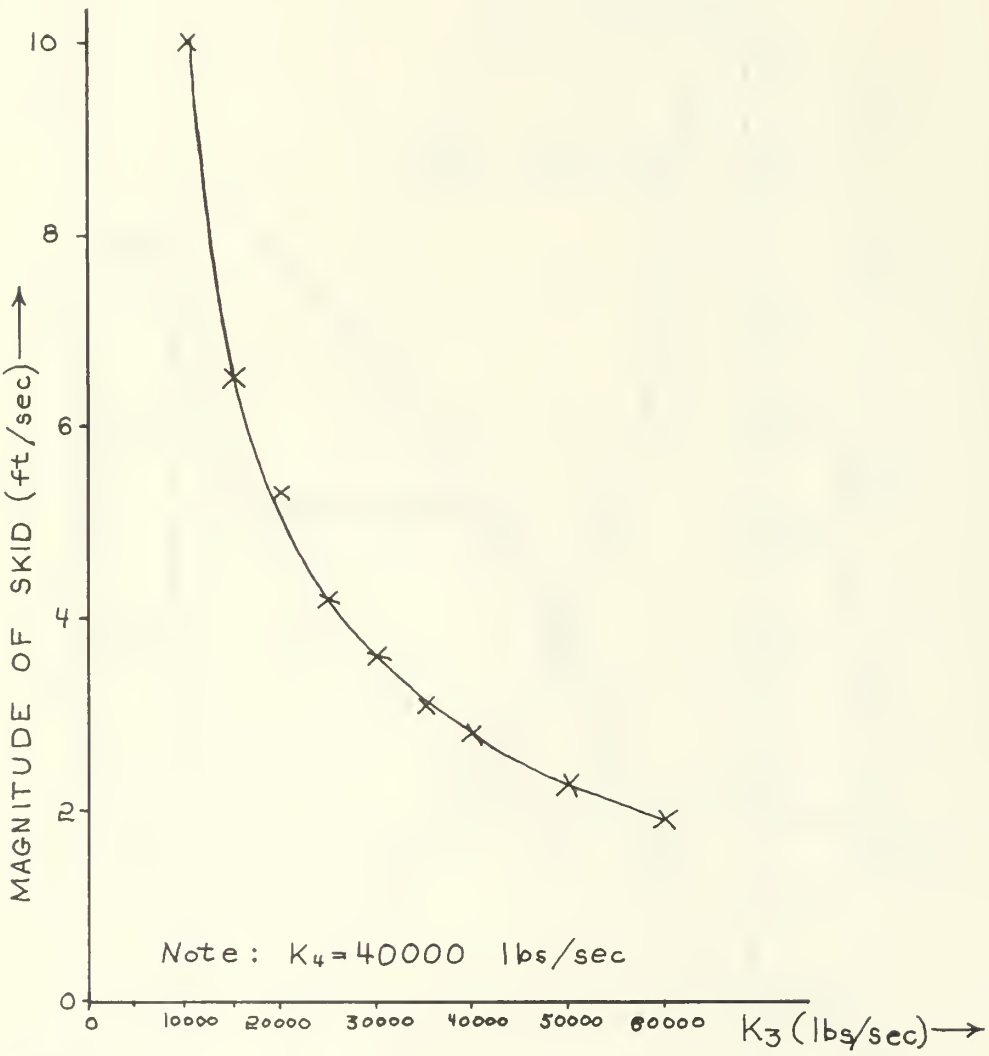


**Fig. 20. Magnitude of skid versus $K_3$ for the double ramp control.**

or $K_4$, since, as mentioned previously, the greater the proportion of the total stop time that is free from a skid, then the greater will be the actual time when the deceleration is less than that experienced when a skid is present.

Even though the double ramp control has serious defects, it nevertheless represents a decided improvement over the completely uncontrolled braking represented in Fig. 14. Since under many road conditions it is the loss of control which occurs when a skid is present that is actually more dangerous than the increase in the stop time, then the double ramp control would have certain merits. The double ramp control is capable of minimizing the skid time and the magnitude of the skid, at a cost of slightly increased stopping distance.

If it is assumed that the stop time, the skid time, and the degree of skid experienced are of equal importance in judging the overall goodness of a particular type of control, then a performance factor (P.F.) can be defined for the uncorrected case, the double ramp control, and for subsequent controls to be tried. This performance factor is defined as the reciprocal of the product of the actual stop time minus the optimum stop time, the skid time, and the degree of skid experienced. The degree of skid will be measured after the velocity has decreased below 60 ft/sec., since that is the velocity below which the value for $\mu$ (between the brake drum and brake shoe) is a constant. The optimum stop time is 3.13 sec.

This definition of a performance factor must not be taken to be the absolute criterion for judging a control and can only be used as a rough guide to determine the relative merits of different

types of controls. It cannot, for example, be used to determine the proper setting of control parameters to give the ideal stopping conditions, since the optimum settings for one set of road conditions might very possibly be different from the optimum settings for another set of road conditions. Also, no account is taken, in the definition of a performance factor, of the fact that a slight degree of skidding might be much less significant than a larger degree of skidding, or that an increase in the stop time might be permissible under some circumstances but entirely unacceptable under others. Nevertheless, the definition given above is convenient and useful, within limits.

For the uncorrected situation of Fig. 14, a performance factor can be computed in order to provide a basis for comparison. The integral of the error curve, rather than the product of the error times the skid time, is used, multiplied by the total stop time minus the optimum stop time. This gives a performance factor of 0.00214 for the completely uncontrolled situation.

For the double ramp control, the values of the performance factor range from 0.0154 to 0.298, and the variation of P.F. with a change in $K_3$ is shown in Fig. 21. This figure is presented only to indicate the trend of P.F. for the double ramp control and not as an aid to selecting the "best" value for $K_3$. However, based on the indication given by the performance factors for the double ramp control, the double ramp control provides a definite overall performance of the system, when compared to the uncontrolled situation.

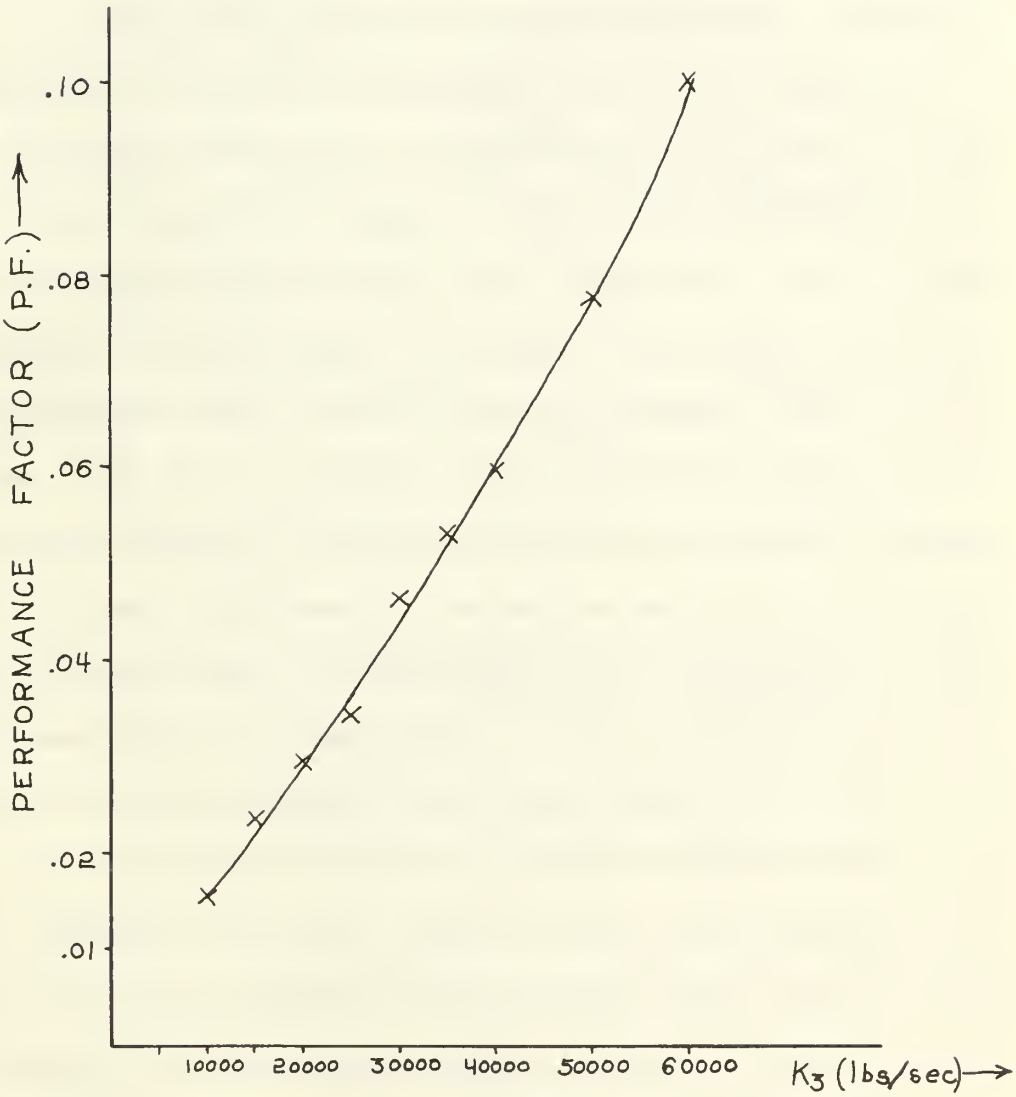


**Fig. 21. Performance factor versus $K_3$ for the double ramp control.**

## 6. THE BANG-BANG CONTROLS.

The bang-bang control with a dead zone was simulated on the analog computer. The dead zone was arbitrarily set at 7.5 ft/sec., which is rather high for a physical system, but which nevertheless serves to illustrate the behavior of the system under this form of control. The response obtained is shown in Fig. 22.

The stop time is seen to be 4.50 sec., which is slightly less than that obtained for the completely uncontrolled situation. This is a predictable result, since for almost the entire cycle the vehicle is in a "controlled" skid, where the term "controlled" implies that the value of the skid is never permitted to exceed a certain value. The reason for the slightly lower stop time than that observed for the uncontrolled situation is that for a small, non-zero time interval in the region where $F_c$ drops to zero and F rises to $F_{in}$, the value of the skid is essentially zero (or at any rate less than the threshold established for detection of an error on the basic system of Fig. 7). While the skid is this small, the coefficient of friction controlling the deceleration of the vehicle is $\mu_s$ (which is greater than $\mu_K$), and the deceleration is thus greater for this small time interval. Since this phenomenon occurs every time the skid is corrected, the cumulative effect over the entire stopping distance is to decrease the stop time slightly.

The major disadvantage to this form of control is the fact that a skid, even though of a small value, is almost always present until the vehicle comes to a complete stop. This also implies that the shortest possible stop time is nearly 4.64 sec., i.e., the same time required to stop when no corrective force is present. However,

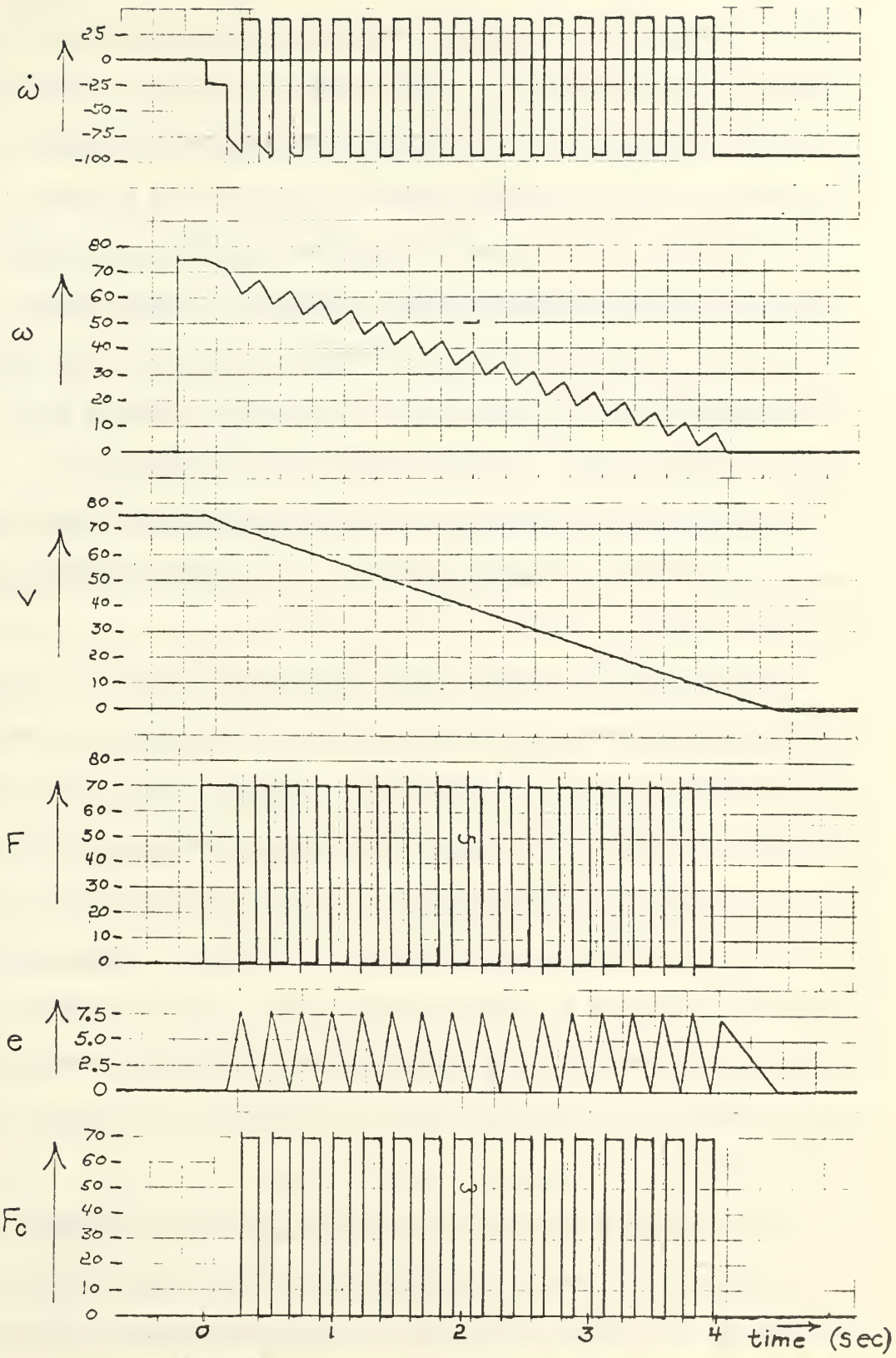


**Fig. 22. Response for the bang-bang control with a dead zone.**

the fact that the skid is controlled, and can theoretically be reduced to an arbitrarily small positive value (by reducing the dead zone) indicates that even this form of control is superior to the uncontrolled situation. An additional advantage is that as the degree of skid is reduced toward 0, i.e., as the relative velocity between the tire and road surface is reduced, the coefficient of friction becomes somewhat greater than that present when a more significant relative velocity is attained. This means that a greater value of deceleration is possible when the skid becomes extremely small. This feature of the coefficient of friction was not incorporated in these analog computer simulations due to the greatly increased complexity of the simulation that would be necessitated.

Even though this control could theoretically provide good performance if the dead zone were reduced sufficiently, there is a serious physical limitation that prevents this from ever really being possible. A little reflection will reveal that the lower the dead zone setting, the more rapidly will the corrective force be required to go on and off. As the dead zone approaches zero, the shape of the corrective force will appear as a high speed oscillation, and the practical lower limit for the dead zone will be determined by both the speed of response of the hydraulic or pneumatic lines and the physical strength of the brake system.

Thus, from a practical point of view, this system appears to offer the advantage of a controlled skid, plus a shorter stop time than that provided by the double ramp control. The disadvantage is that a skid is almost always present, and the level to which it could be reduced would be severely limited by the physical response of the brake lines.

Neither control tried thus far appears to be superior to the other. This is verified somewhat by determining the performance factor for the bang-bang control with a dead zone. The performance factor (computed by taking the reciprocal of the product of the integral of the error and the difference between the stop time and the optimum time to stop) is determined to be 0.046. This is neither significantly better nor worse than any of the performance factors obtained for the double ramp control.

The bang-bang control with a time delay was then simulated. The results for this simulation are presented in Fig. 23. A time delay of 0.1 sec. (problem time) was chosen for this simulation. The stop time is seen to be 5.93 sec., which is considerably worse than the stop time for the previously described bang-bang control. However, in this case the skid is eliminated for a portion of the total stop cycle, and the skid time is 3.92 sec. Superficially this appears to be an improvement over the previous bang-bang control, but closer examination reveals that very little, if any, betterment of the performance is gained by the incorporation of a time delay.

Reference to Fig. 24, which is an expansion of a portion of Fig. 23, and was obtained by manual solution of simplified equations of motion, reveals that for a significant period of time during each error correcting cycle the velocity remains a constant. For example, from point (2) to (3) , where no skid is present, the velocity is also a constant. The time from (2) to (3) is 0.1 sec., and corresponds to the time delay built into the corrective force. During this time, the net force F on the brake shoe is zero, and thus the velocity remains constant. If the time delay is decreased, this control

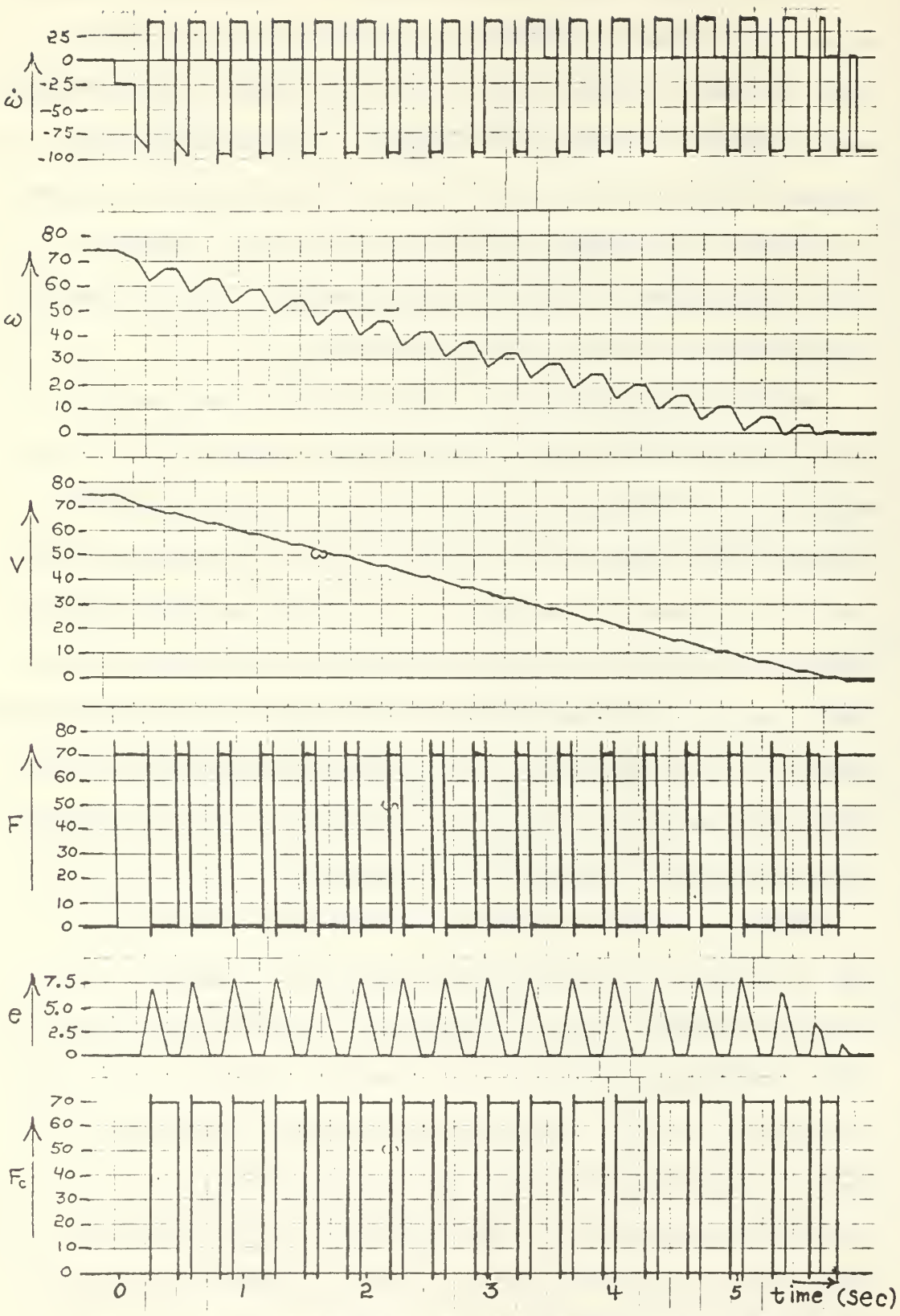


Fig. 23. Response for the bang-bang control with a time delay.

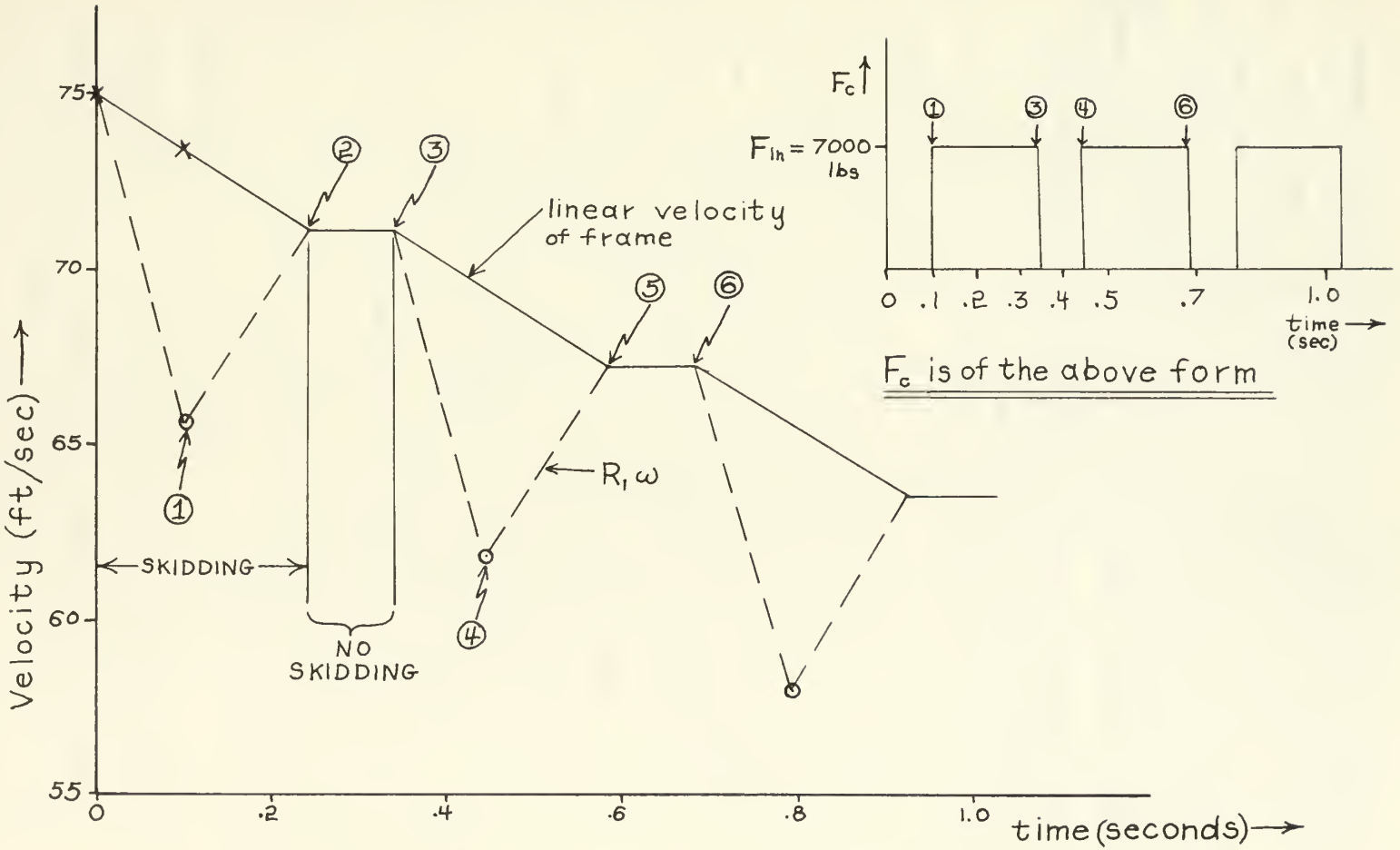


**Fig. 24. Expanded plot of wheel velocity and vehicular velocity versus time for the bang-bang control with a time delay.**

approaches the performance of the bang-bang control with a zero dead zone.

The bang-bang control with a time delay thus appears superior to a completely uncorrected braking situation, but appears somewhat inferior to either of the two controls previously described. A performance factor for this control (for the specific set of parameters used for this simulation) is 0.025, which is sufficiently lower than the trend of the values obtained for the previous two controls to warrant the above conclusion.

## 7. THE TRIPLE RAMP CONTROL.

The triple ramp control of Fig. 12 was the final type of corrective scheme to be implemented. A total of 100 separate computer runs were made, using a variety of values for the parameters $K_3$, $K_4$, $K_c$ and C.R. (correction ratio). Representative samples of the behavior to be expected from this type of corrective scheme are shown in Fig. 25 and Fig. 26.

The most striking features about both Fig. 25 and Fig. 26 are the low stop time, skid time, and magnitude of error present for this form of control. For example, Fig. 25, with $K_3$ = 60000 lbs/sec., $K_4$ = 40000 lbs/sec., $K_c$ = 1000 lbs/sec. and C.R. = 2.05 has a stop time of 4.22 sec., skid time of 0.98 sec. and roughly 1.9 ft/sec. as the degree of skid. This gives a performance factor of 0.493 which is higher than the maximum value attained for any control tried previously. This value of performance factor is of course affected by the values of the various parameters $K_3$, $K_4$, $K_c$, and C.R., and does not represent the "best" value of P.F. that was obtained on the trial runs for the triple ramp control. Indeed, the term "best" is misleading here, since a setting of parameters resulting in the highest possible P.F. would sacrifice an adaptability to changing road conditions. This feature will be discussed more thoroughly later in this paper.

Nevertheless, it can be concluded from the above factors and an inspection of Fig. 25 and Fig. 26 (along with the Author's analysis of the other 98 analog computer runs) that the triple ramp control provides more nearly optimal braking conditions than any previously described control.

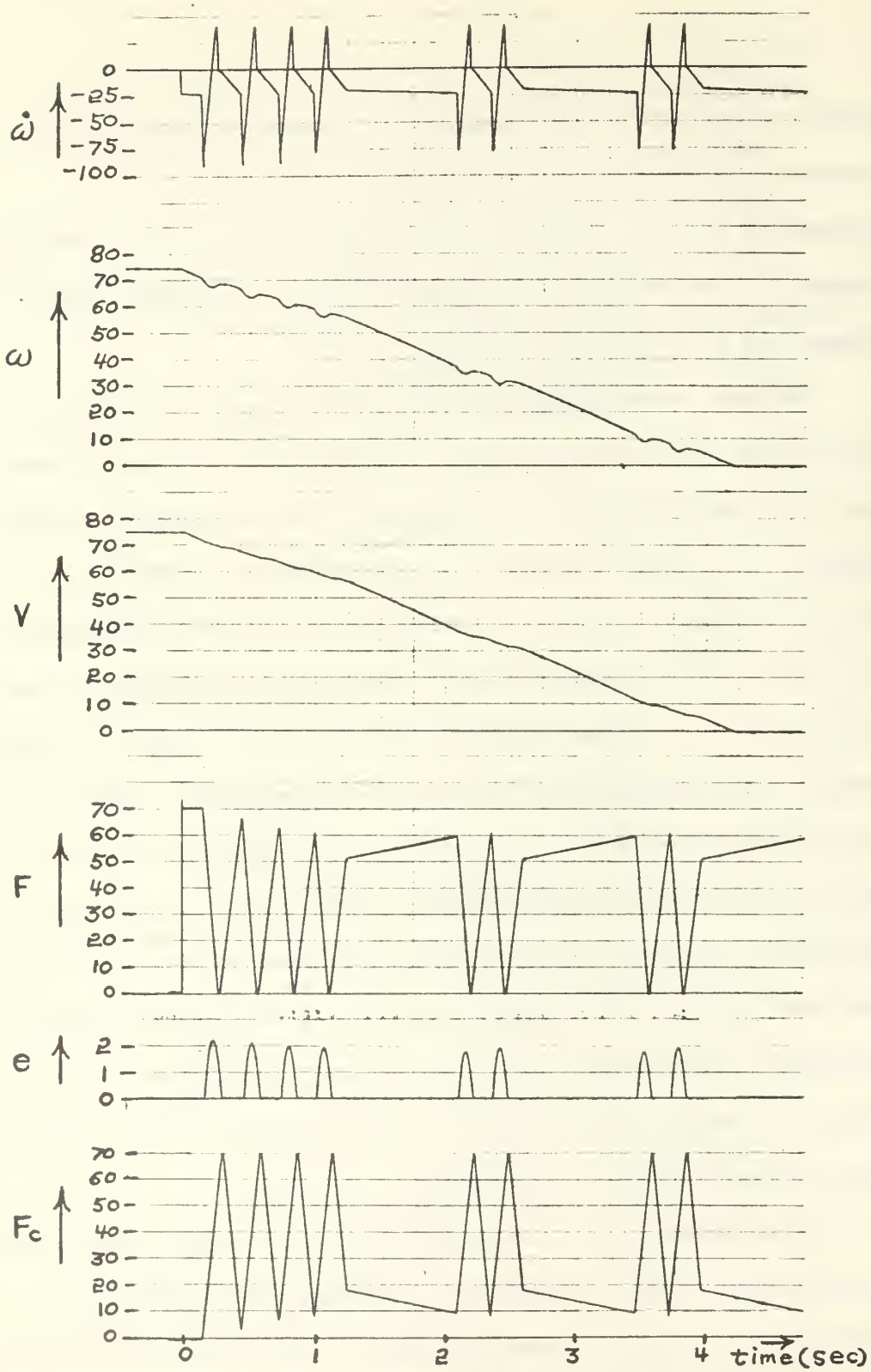


Fig. 25. Triple ramp control response, $K_3$ = 60000 lbs/sec., $K_4$ = 40000 lbs/sec., $K_c$ = 1000 lbs/sec., C.R. = 2.05

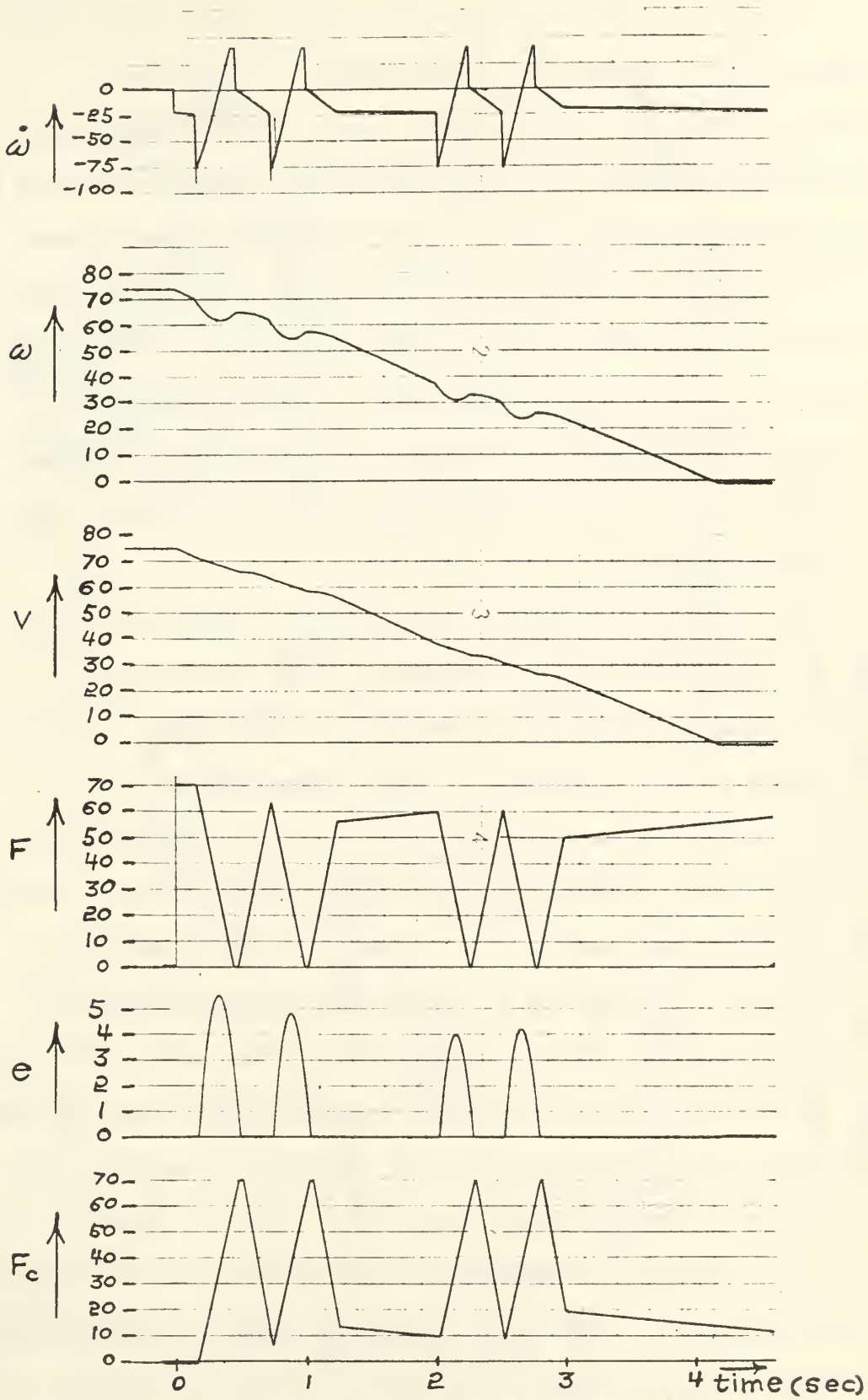


Fig. 26. Triple ramp control response, $K_3$ = 25000 lbs/sec., $K_4$ = 25000 lbs/sec., $K_c$ = 500 lbs/sec., C.R. = 2.05.

A closer examination of the actual behavior of this triple ramp control is appropriate at this point. The results of a manual solution of the equations of motion (with the simplifying assumptions mentioned previously for similar hand calculations) are presented graphically in Fig. 27. The parameter values assumed were $K_3$ = 50000 lbs/sec., $K_4$ = 80000 lbs/sec., $K_c$ = 1000 lbs/sec., and C.R. = 1.5. Also, the coefficient of friction $\mu$ between the brake drum and brake shoe was assumed to be constant at 0.8 for the hand calculation (this was the only simplifying assumption). All other conditions were assumed the same as previously listed for other simulations.

An examination of Fig. 27 indicates that from time = 0 sec. to the point marked (5) , the behavior of the control and the vehicle response are precisely analogous to the double ramp form of control. This can best be seen by a comparison of Fig. 27 with Fig. 17 over the region from time = 0 sec. to the point (5) . The same defect present in the double ramp control is also present in the triple ramp control, i.e., from point (2) to point (3) the velocity is decreasing at a rate slower than the rate of deceleration when a skid is present. Also, from point (5) to point (6) this phenomenon occurs. However, at point (7) , when the downward slope of the corrective force $F_c$ abruptly changes from - $K_4$ to - $K_c$ the situation changes completely. While the slope of $F_c$ = - $K_c$, the rate of decrease of the velocity not only is significantly greater than that possible during a skid, but also no error is present until the value of the deceleration again exceeds - 24.0 ft/sec.$^2$ at point (8) . At this time the process repeats itself.

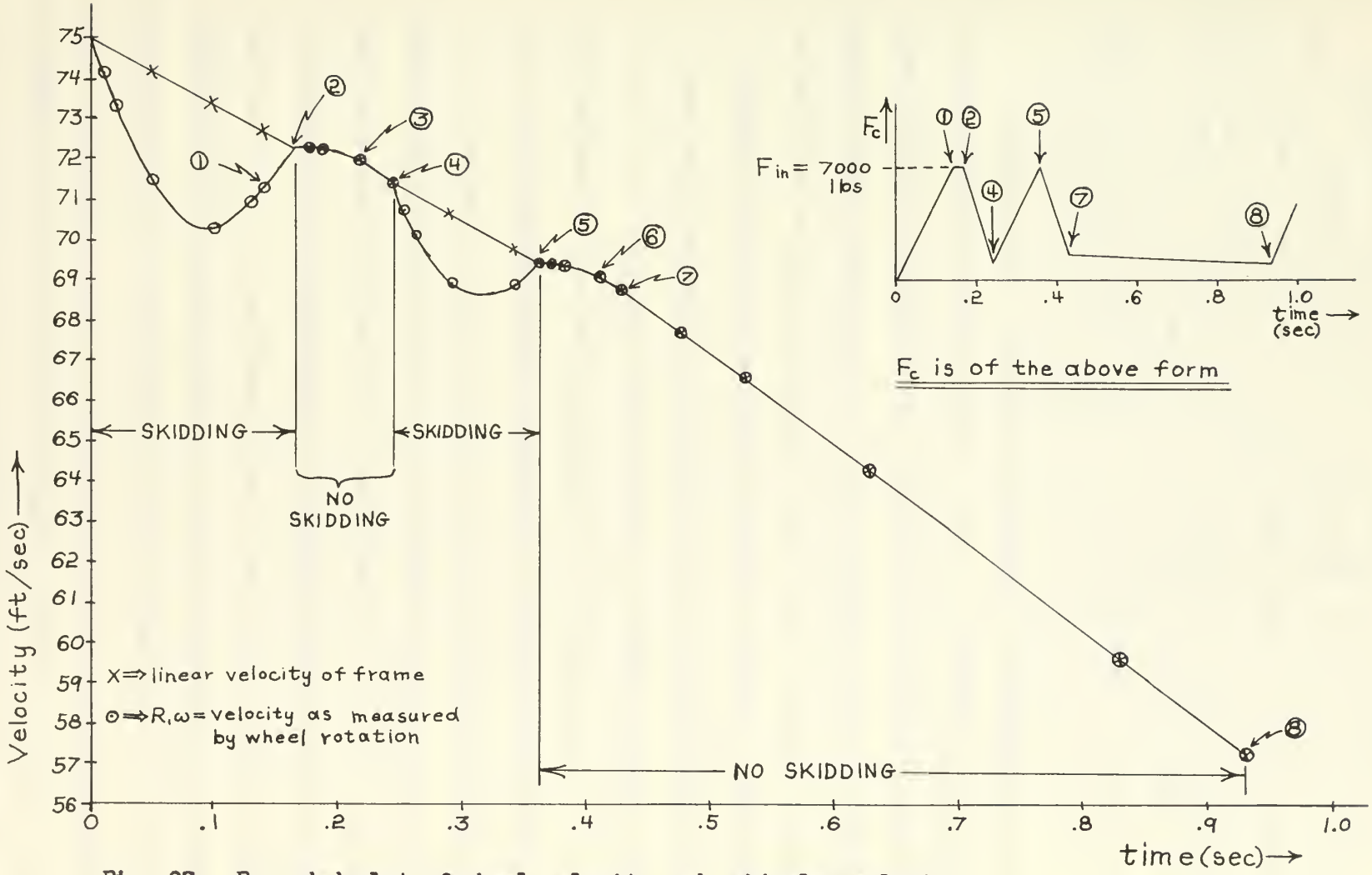


**Fig. 27. Expanded plot of wheel velocity and vehicular velocity versus time for the triple ramp control.**

It is during this last phase of the skid correcting cycle (from point ⑦ to point ⑧ in Fig. 27) that the inherent superiority of the triple ramp control is manifested. During this portion of the cycle the deceleration is gradually increasing as $F_c$ slowly decreases. When the deceleration is too great for the prevailing road conditions a skid once again occurs, but prior to this occurrence of the skid the deceleration is more and more closely approaching the optimum deceleration. Additionally, if the road conditions are changing, for example, if the vehicle went from a patch of slick pavement to dry pavement, and the coefficient of friction between the tire and road surface were increased, then this form of control permits the deceleration to increase to the new optimum value. In other words, the triple ramp control is continually sampling the road conditions and permitting the braking force to adapt to changing road conditions.

The desirability of this adaptability feature is evident. It is also apparent that for the invariant road conditions simulated for this problem, the most nearly ideal braking situation would have been achieved by setting C.R. to a value just slightly greater than one, and causing $K_c$ to equal zero. This would have permitted only two skids of small magnitude to occur, and for the remainder of the path the vehicle would have slowed down at a rate very nearly equal to the optimum deceleration. This would provide a very large value for the performance factor, which would of course be a misleading indication in this case, since the control would not respond to improved road conditions. It would, however, still respond to worsening road conditions, so there is even some merit in this proposal.

Referring back to Fig. 25, we note that the typical triple ramp shape of $F_c$ does not become evident until after the occurrence of the fourth error signal, whereas in Fig. 26 the triple ramp shape appears as expected after the occurrence of the second error signal. Recall that the form of the coefficient of friction $\mu$ between the brake drum and brake shoe is given by

$$\mu = .8 - .01\ (\omega - 60) \text{ for } \omega > 60 \text{ rad/sec.}$$

Reference to the $\omega$ versus time plot of Fig. 25 reveals that both the first and second errors occur while the rotational velocity is above 60 rad/sec. Thus in this region the value for $\mu$ is constantly changing in accordance with the above relation. Now, when the first error signal (or skid) is sensed the corrective force $F_c$ immediately increases until the skid is eliminated, and then decreases until the skid occurs once more; this value of $F_c$ at which the skid occurs is stored by a storage device. Upon the occurrence of the second skid, $F_c$ increases again until the skid is once more eliminated. Ideally the value of $F_c$ should drop to some multiple of the stored previous value of $F_c$ (the multiple being established by C.R.). However, the velocity of the vehicle is decreasing continually during this process and $\mu$ is thus increasing. This means that after the occurrence of the second skid, the net torque on the wheel for a given value of $F_c$ (e.g., for a value equal to C.R. times the previously stored value of $F_c$) is now greater than it would be if the value for $\mu$ were not increasing. Thus a third skid occurs before $F_c$ can drop to the value at which the break point occurs. However, after the occurrence of the fourth skid, $\mu$ is constant, and thus the typical triple ramp effect is observed.

In Fig. 26 the above phenomenon does not occur. Note that in this figure the value of $K_3$ is only 25000 lbs/sec. whereas in Fig. 25 $K_3$ had a value of 60000 lbs/sec. This means that the error will be corrected more slowly, and thus the velocity will have decreased to a level where $\mu$ is a constant by the time the second error has been eliminated. Thus the coefficient of friction will not have changed sufficiently between the time when the value of $F_c$ was stored and the time when $F_c$ reaches its break point to cause another error signal to occur. Note, however, that if C.R. had been set sufficiently low (e.g., slightly above 1.0) then the same phenomenon that occurred in Fig. 25 would also have occurred in Fig. 26. Conversely, had C.R. been set sufficiently high, this phenomenon would not have occurred in Fig. 25.

Figure 28 presents a plot of stop time versus $K_c$, with C.R. as a parameter. The data points on this and subsequent plots were obtained from the graphical output resulting from the various analog computer runs made while simulating the triple ramp control. Consequently, the accuracy of the individual data points is only of the order of a few percent. However, this degree of accuracy is sufficient to demonstrate the overall performance characteristics of the triple ramp control quite satisfactorily. From Fig. 28 we can see that as $K_c$ increases the stop time increases also. However, the rate of increase, i.e., the slope of the curve, is observed to be a variable, even though the overall trend is upward. This overall upward trend is expected in view of previous comments concerning the adaptability feature inherent in the triple ramp control. A decrease in stop time must be achieved at the cost of a decrease in

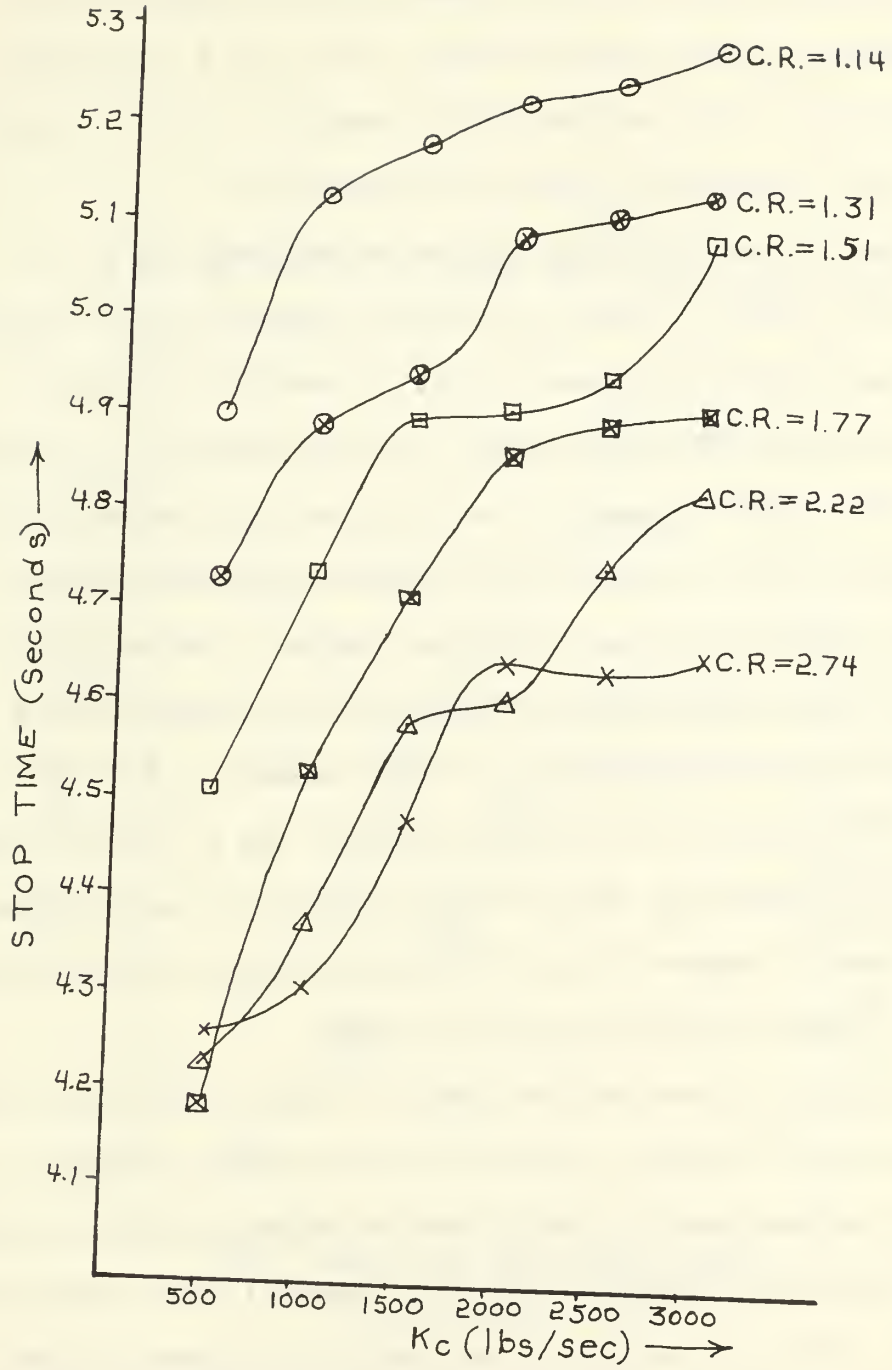


**Fig. 28. Stop time versus $K_c$ with C.R. as a parameter for the triple ramp control.**

the sensitivity of the control to improving road conditions, all other parameters being assumed constant. Thus, as $K_c$ increases, the vehicle goes into a skid mode more frequently, and the overall trend of stop time with $K_c$ would be an upward one.

However, to satisfactorily account for the leveling off of the stop time versus $K_c$ chart at localized regions, we must investigate the detailed behavior more closely. Figure 29 is a plot of both stop time and skid time versus $K_c$ for one specific set of parameters. The numbers adjacent to the skid time curve represent the total number of skids present in the particular graphical output from which each specific data point was obtained. For example, 8 skids were present in the analog computer output obtained with a setting of $K_3$ = 60000 lbs/sec., $K_4$ = 25000 lbs/sec., C.R. = 2.05, and $K_c$ = 1500 lbs/sec. For $K_c$ = 2500 lbs/sec. and $K_c$ = 3000 lbs/sec., 10 skids were present and the skid time was thus the same for each of these values. However, Fig. 29 also reveals that the stop times for each of these values of $K_c$ were the same.

In a situation where the same number of skids is observed from one value of $K_c$ to another, then the skid times will obviously be identical, assuming that $K_3$ (which directly determines the magnitude of each skid and the length of time it is present) is the same for each trial. The only factor contributing to a difference in overall stop time is thus the difference in time between adjacent pairs of skids (e.g., the time from point (5) to point (8) in Fig. 27). For a larger value of $K_c$, the time between pairs of skids is decreased. Now, for example, when 10 skids occur for a value of $K_c$ = 3000 lbs/sec. the time between adjacent pairs of skids is shorter than the time between the adjacent pairs of 10 total skids obtained for $K_c$ = 2500

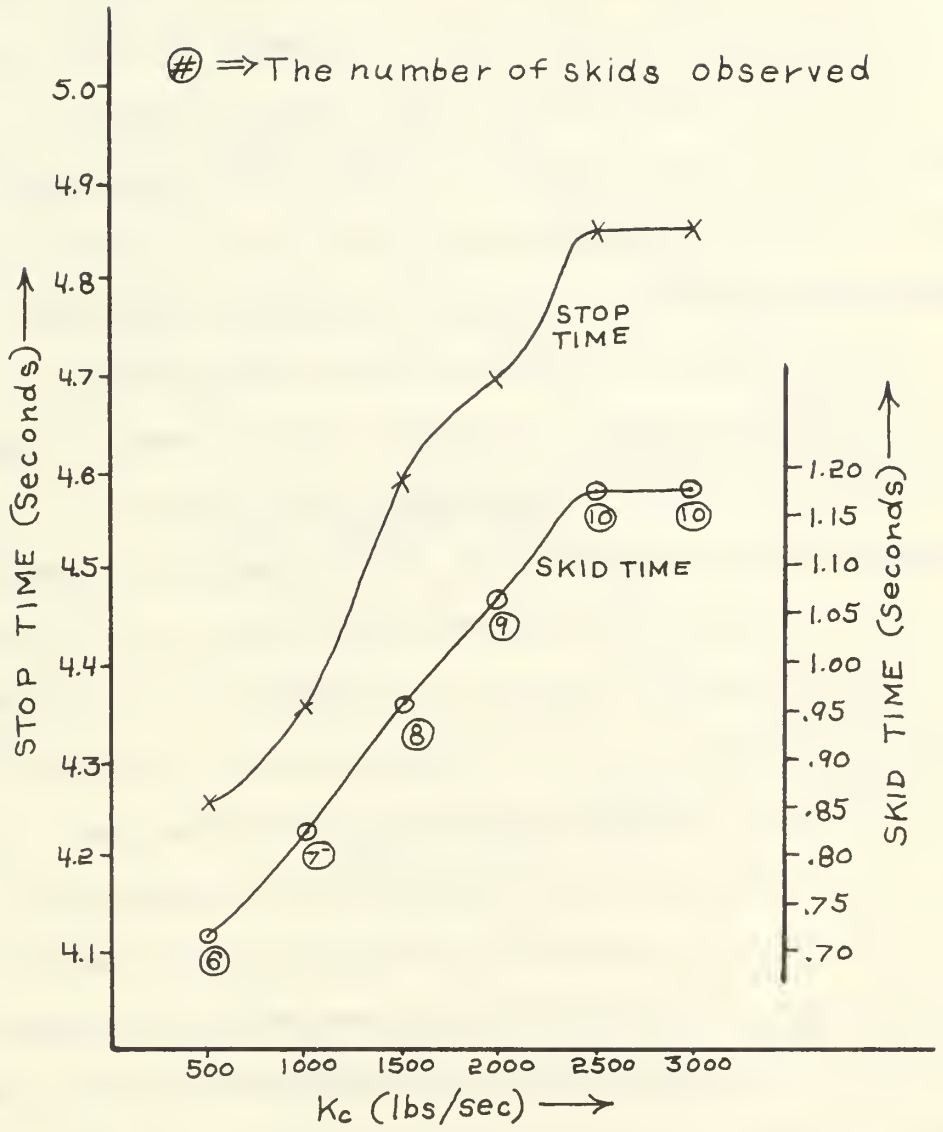


**Fig. 29. Skid time and stop time versus $K_c$ for the triple ramp control, $K_3$ = 60000 lbs/sec., $K_4$ = 25000 lbs/sec. C.R. = 2.05.**

lbs/sec. Thus the final pair of skids occurs earlier when $K_c$ = 3000 lbs/sec., but due to a larger value of $K_c$ a larger value of deceleration is attained after the tenth skid and prior to the vehicle coming to a complete stop. There is also a longer period of time after the tenth skid occurs, during which the slope of $F_c = - K_c$, for the case where $K_c$ = 3000 lbs/sec. These two factors serve to account for the leveling off of the stop time versus $K_c$ curves observed for Fig. 28 and Fig. 29. It is also possible that a slight local decrease in total stop time might occur for an increase in $K_c$ under the proper combination of control parameters and road conditions. This is observed in Fig. 28 in one region of the curve obtained for C.R. = 2.74.

Despite the above observations, the conclusion to be drawn from Fig. 28 and Fig. 29 is that the overall effect of an increase in $K_c$ is to increase the stop time of the vehicle, and to degrade the overall performance of the corrective system. A compromise must thus be reached between adaptability to improving road conditions and decreasing the total stop time. Designing for a worst case situation, a satisfactory value for $K_c$ would thus be $K_c$ = 500 lbs/sec., as this would permit reasonably rapid response to improving road conditions while still providing very good braking performance under nearly static road conditions.

The next parameter to be investigated is the correction ratio (C.R.). Figure 30 is a plot of the stop time versus the correction ratio, with $K_c$ as a parameter. The overall trend as determined from Fig. 30 is that the stop time tends to decrease with an increase in the value of C.R. Each curve in the family of Fig. 30 demonstrates

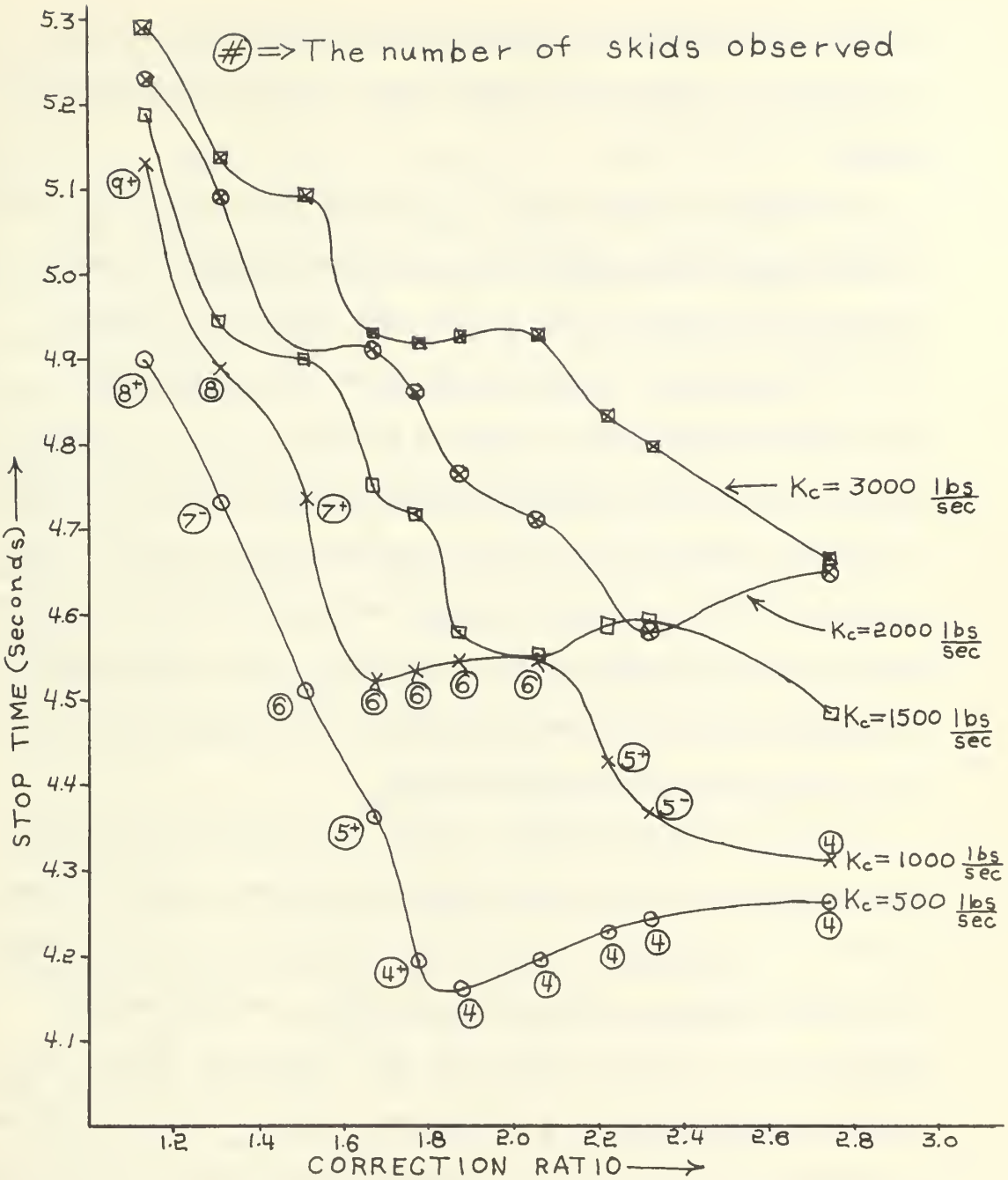


**Fig. 30. Stop time versus C.R. with $K_c$ as a parameter for the triple ramp control.**

notable local exceptions to this trend, however, and, as will be pointed out, excessively large values of C.R. will materially lengthen the stop time.

The overall downward trend of the stop time versus C.R. curve is best understood by referring to the inset of Fig. 27, where a pictorial description of the triple ramp control is presented. As the value of C.R. is raised this raises the break point at which the transition of the slope of $F_c$ from $-K_4$ to $-K_c$ occurs. This has the effect of lengthening the time between the occurrence of adjacent skid pairs, since the time that $F_c$ will take to drop to the level where a skid will occur once more increases in direct proportion to the height of the break point. It is thus seen that increasing C.R. has the same net effect as decreasing the value of $K_c$, with certain minor restrictions.

It would be expected that, as C.R. is increased to obtain a set of braking histories, those output traces which have the same number of skids present for differing values of C.R. would behave in a manner similar to that observed when $K_c$ was the variable quantity (e.g., in Fig. 28 and Fig. 29). Referring in Fig. 30 to the curve obtained for $K_c$ = 500 lbs/sec., we see that the stop time increases with increasing C.R. when the total number of skids present in each braking history remains a constant four (this is also observed for $K_c$ = 1000 lbs/sec., for six skids observed). The reason for this is very simple. As C.R. is raised this "pushes" the adjacent pairs of skids farther apart and thus for a larger portion of the total stop time the vehicle is decelerating at a lower rate than if C.R. were set lower. Thus if the total of skids still remained the

same, the control which provided the greater deceleration over the entire skid free path would also provide a shorter stop time. This is the control with the lower C.R.

Note that C.R. is also closely linked to the adaptability of the system to improving road conditions, since for a large value of C.R. the time required for $F_c$ to drop (at a rate of $- K_c$) to a level where the road is "tested" for better conditions is lengthened. Additionally, C.R. cannot be increased to a very large value without greatly extending the stop time. The minimum number of skids possible (starting with any significant initial velocity) is two. Once C.R. has been increased to a level where only two skids are present, then any further increases in C.R. will cause a rapid increase in the stop time for the reasons listed in the preceding paragraph. However, long before the skids were reduced to two in number, the stop time would also have increased due to the low value of deceleration that would be present over an excessively large portion of the vehicle's trajectory.

In retrospect, it appears that despite the downward trend of stop time with increasing C.R. presented in Fig. 30, any advantages to be gained by very large values of C.R. are outweighed by the disadvantages. On the basis of information presented here, a "safe" value for C.R. would appear to be about 2.0.

Figure 31 and Fig. 32 present plots of both stop time and skid time versus C.R. for two different sets of parameters. They are included primarily for information, the most significant factor about either one being that where the curve representing skid time becomes flat (implying a constant number of skids were observed for

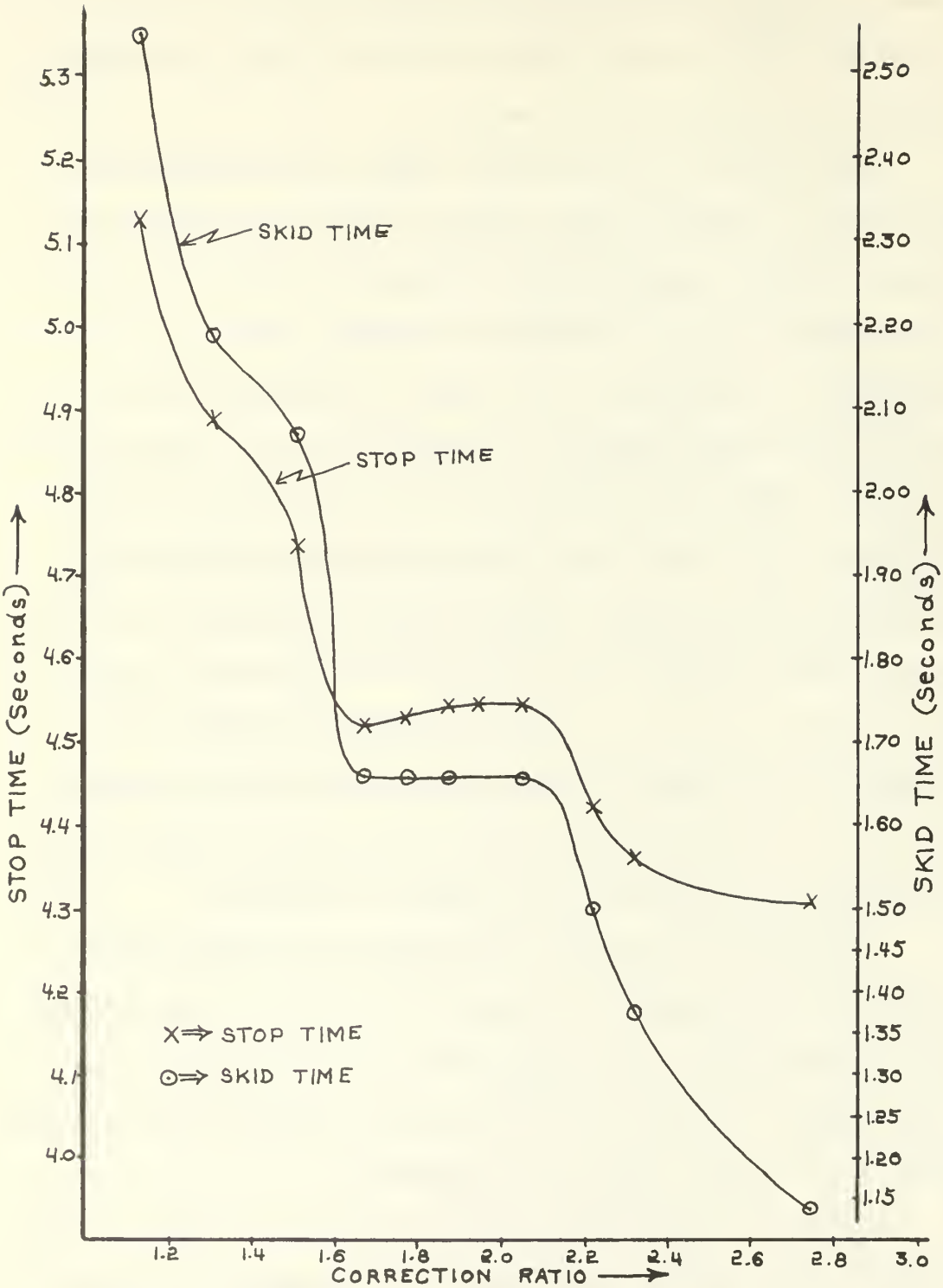


**Fig. 31. Stop time and skid time versus C.R. for the triple ramp control, $K_3$ = 25000 lbs/sec., $K_4$ = 25000 lbs/sec., $K_c$ = 1000 lbs/sec.**

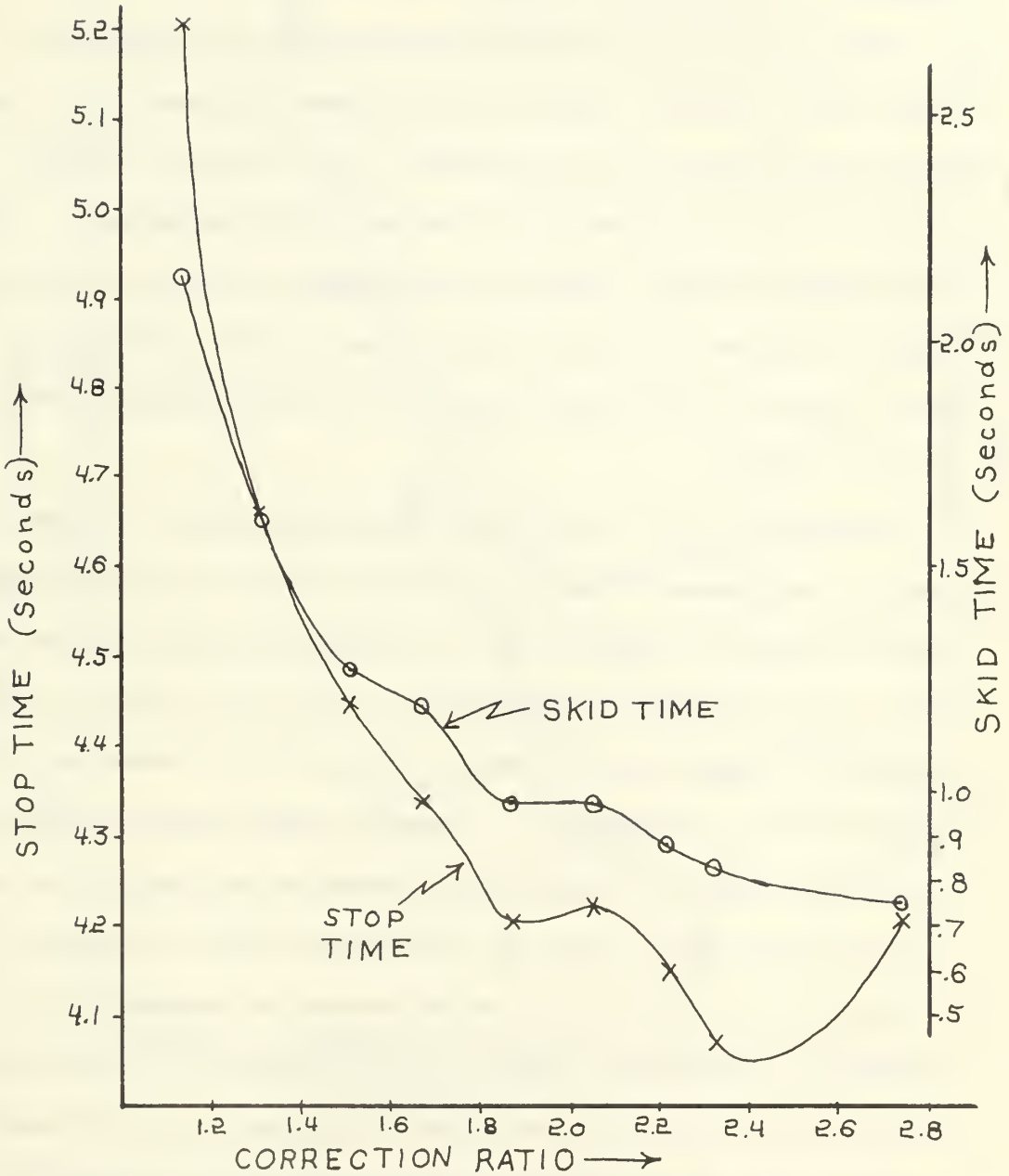


**Fig. 32. Stop time and skid time versus C.R. for the triple ramp control, $K_3$ = 60000 lbs/sec., $K_4$ = 40000 lbs/sec., $K_c$ = 1000 lbs/sec.**

succeeding braking history plots) the curve for stop time acquires a positive slope. This serves to reinforce the arguments previously advanced.

The behavior of the braking performance as $K_3$ is varied is also of some interest. Figure 33 illustrates the behavior of stop time and skid time as $K_3$ is increased. Notice that the tendency exhibited is for the stop time to decrease with increasing $K_3$. This is the expected result, since the larger the value of $K_3$, the more rapidly is any error or skid corrected back to zero, and thus a larger portion of the braking path will be in a controlled mode of skid free braking.

Referring back to Fig. 27 once more, we note that the time from the commencement of braking action ($t = 0^+$) to point ① , and also from point ④ to point ⑤ , is dependent solely upon the value of $K_3$, whereas the time from point ② to point ④ and from point ⑤ to point ⑧ depends upon $K_4$ and $K_c$. Thus as $K_3$ is increased the total skid time and magnitude of each individual skid are reduced. This has the effect of causing each successive skid pair to occur earlier in time, even though the time between skids is unchanged. As long as the total number of skids present is unchanged as $K_3$ is increased, an improvement will always be observed in the stop time. However, in the event that one value of $K_3$ causes a certain number of skids, and a higher value of $K_3$ is just sufficient to increase the number of skids, then a slight local increase will be observed in the stop time. This phenomenon is seen to occur in Fig. 33. The explanation for this is as follows. When $K_3$ = 50000 lbs/sec. the time remaining between the correction of the sixth skid and the complete stopping of the vehicle is insufficient for the deceleration

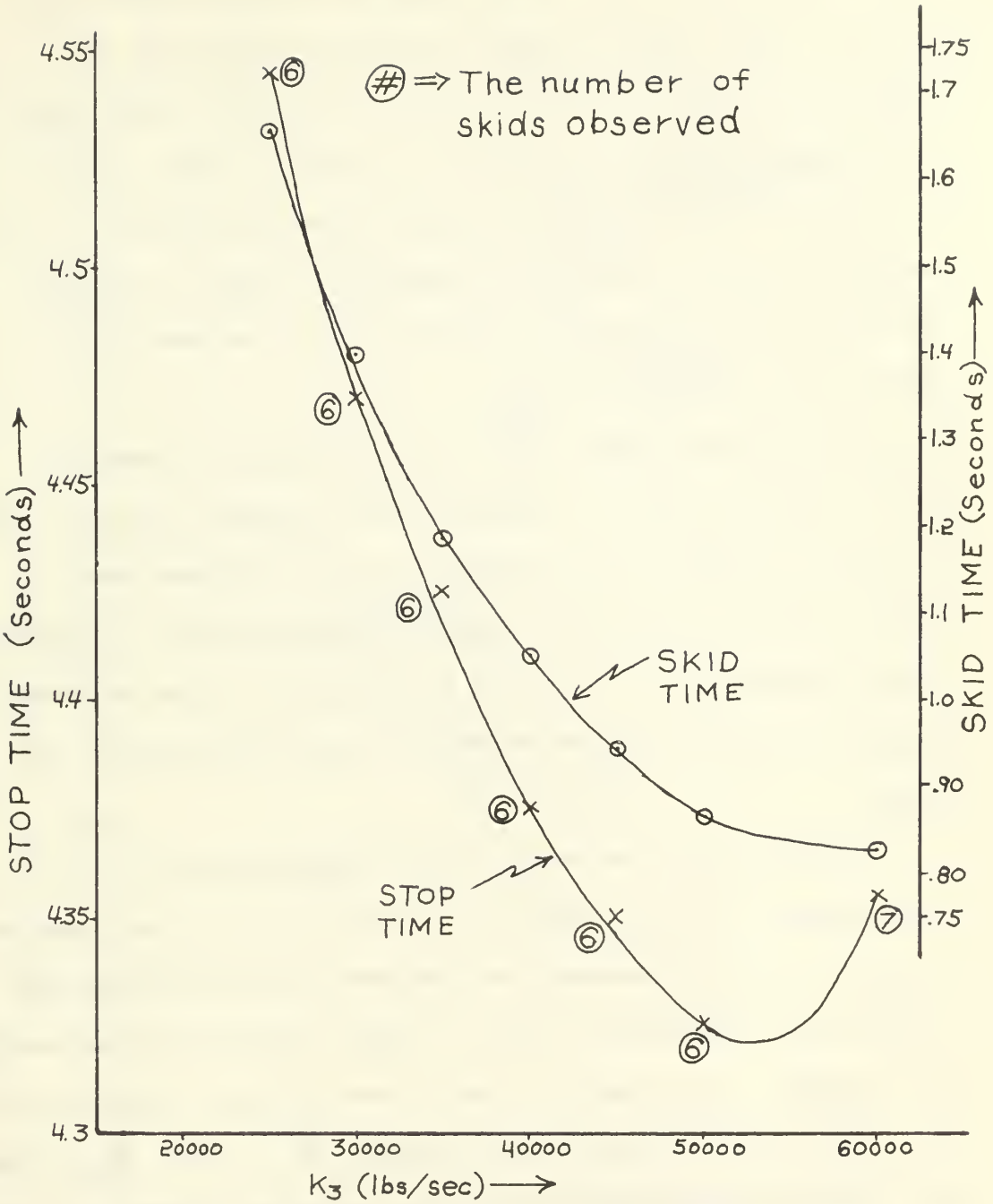


Fig. 33. Stop time and skid time versus $K_3$ for the triple ramp control, $K_4$ = 25000 lbs/sec., $K_c$ = 1000 lbs/sec. C.R. = 2.05

to have increased to that level necessary to cause another skid. However, for $K_3$ = 60000 lbs/sec. the seventh skid occurs just prior to the vehicle coming to a rest. During this seventh skid the vehicle deceleration is only - 16 ft/sec.$^2$, rather than the - 24 ft/sec.$^2$ that was experienced just prior to the skid. It is this lower value of deceleration present just prior to stopping that causes the stop time to increase as $K_3$ is increased from 50000 lbs/sec. to 60000 lbs/sec.

The above phenomenon is just restricted to the transition points where the number of complete skids increases from one value to another. However, the decreased skid times and magnitude of skids caused by an increased value of $K_3$ indicates that the greatest overall advantage is to be gained by making $K_3$ as large as possible, regardless of any localized increases in stop time caused by this policy.

Finally, the system behavior with changing values of $K_4$ is investigated. Figure 34 indicates that the stop time decreases as the value of $K_4$ is increased, but that the skid time goes up with increasing $K_4$. Reference to Fig. 27 again facilitates understanding this behavior. From Fig. 27 it can be seen that the time lapse from point ② to point ④ and also from point ⑤ to point ⑦ is dependent solely upon the value of $K_4$. Large values of $K_4$ will cause the time intervals between the points to become small, while leaving time intervals along other portions of the trajectory unchanged. Since it is during the time interval from point ⑤ to point ⑥, for example, that the deceleration of the vehicle is even less than that present while in a skid, any factor which will shorten the time

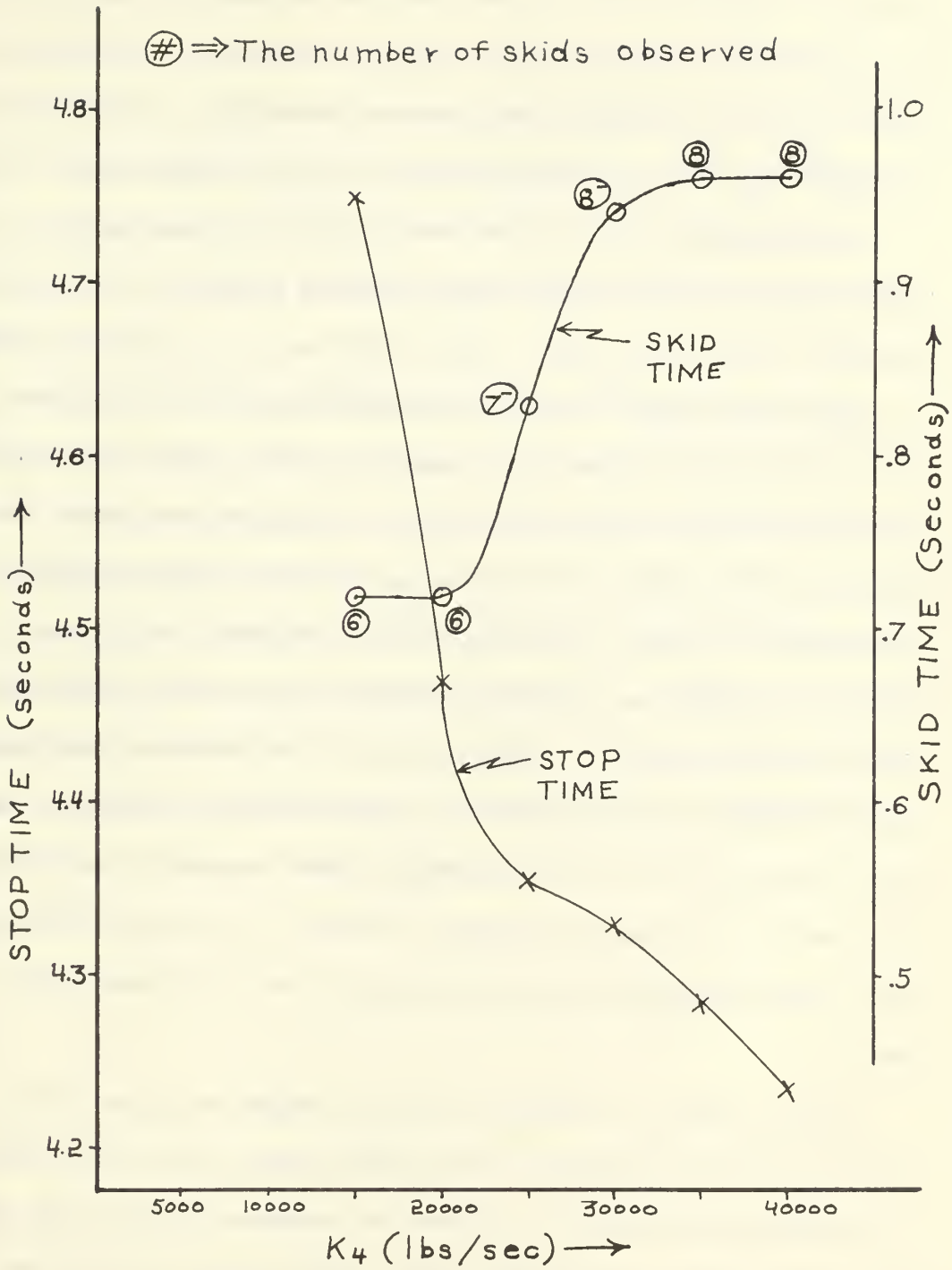


Fig. 34. Stop time and skid time versus $K_4$ for the triple ramp control, $K_3$ = 60000lbs/sec., $K_c$ = 1000 lbs/sec. C.R. = 2.05

from ⑤ to ⑦ will also shorten the time the vehicle spends in the undesirable region from ⑤ to ⑥ . This will naturally cause a shorter stop time, since the vehicle will be decelerating at a high rate over a larger proportion of its stopping path.

The increase of skid time noted in Fig. 34 is once again related closely to the total number of skids present. As the time from ② to ④ or from ⑤ to ⑦ (referring once again to Fig. 27) is reduced, this tends to shorten the time between the occurrence of adjacent skids. If the total number of skids remains the same while $K_4$ is being increased, the skid time naturally remains the same (to fully appreciate this, one must recall that the duration and magnitude of each individual skid is controlled by $K_3$ only, which is not being varied here). However, as the skid occurrences become closer together in time, a point is reached where the total number of skids encountered in the stopping history increases, and thus the skid time will also increase. This increase in skid time would not be a serious consequence, however, if $K_3$ were sufficiently high to make the duration and magnitude of the individual skids very small.

Thus it might be concluded that the larger the value of $K_4$, the better the performance of the entire system, since the decrease in stop time would more than offset any increase in skid time, particularly if $K_3$ were also set very high. Caution must be exercised here, however, because it is the nature of the triple ramp control that the value of $F_c$ at which every second error occurs must be marked and stored. This means that if $K_4$ is too large, then difficulties would be encountered in marking the point at which each second error

occurs, and additionally in reversing the trend of $F_c$ (i.e., in changing from a slope of $-K_4$ to $+K_3$). Obviously a slope of - infinity for $-K_4$ would be totally unsatisfactory. Thus, a very large value of $K_4$ would indeed provide the best performance, but this value must not be so great as to create excessive difficulties in measuring and storing the point at which each second error occurs.

In summary, the following qualitative comments concerning the choice of the values for the various parameters of the triple ramp control are appropriate. $K_3$ should, with no qualifications, be made as large as possible. $K_4$ should also be as large as possible, short of being a negative step function, and subject to the restrictions mentioned in the preceding paragraph. $K_c$ should be relatively low assuming that C.R. is not too large. A value for C.R. of about 2.0, and for $K_c$ of 500 lbs/sec. was determined to be satisfactory for the particular system simulated here.

## 8. PROPOSED IMPLEMENTATION OF THE TRIPLE RAMP CONTROL.

In view of the obvious superiority of the triple ramp form of control over any of the other controls examined, a proposal for the physical implementation of this control is advanced here. It must be assumed that a linear accelerometer of high accuracy and linearity over the range from 0 ft/sec.$^2$ to 32 ft/sec.$^2$ is available. A high gain, broad bandwidth operational amplifier is necessary to provide the integrator used in conjunction with the linear accelerometer (see Fig. 1 for the block diagram of the system). Additionally, an accurate tachometer to measure the rotational velocity of the wheels is assumed to be available. Thus, all elements necessary to accurately register the occurrence of a skid are assumed to be available. Our attention will be directed toward the actual mechanism by which the triple ramp control is generated, and by which the pressure applied to the brake cylinder is modified.

Figure 35 illustrates the means by which it is proposed to implement the triple ramp control. An explanation of Fig. 35 follows.

A force which is applied to the brake pedal is transmitted to the brake drum via the hydraulic lines. Until a skidding situation occurs $V_c$ is held equal to $V_{max}$ by means of the ramp generator and limiter. When $V_c$ equals $V_{max}$, full braking action is applied and no corrective action is occurring.

The first time a skid occurs, e (error) becomes greater than zero, and switches (1) and (2) throw in the indicated manner.

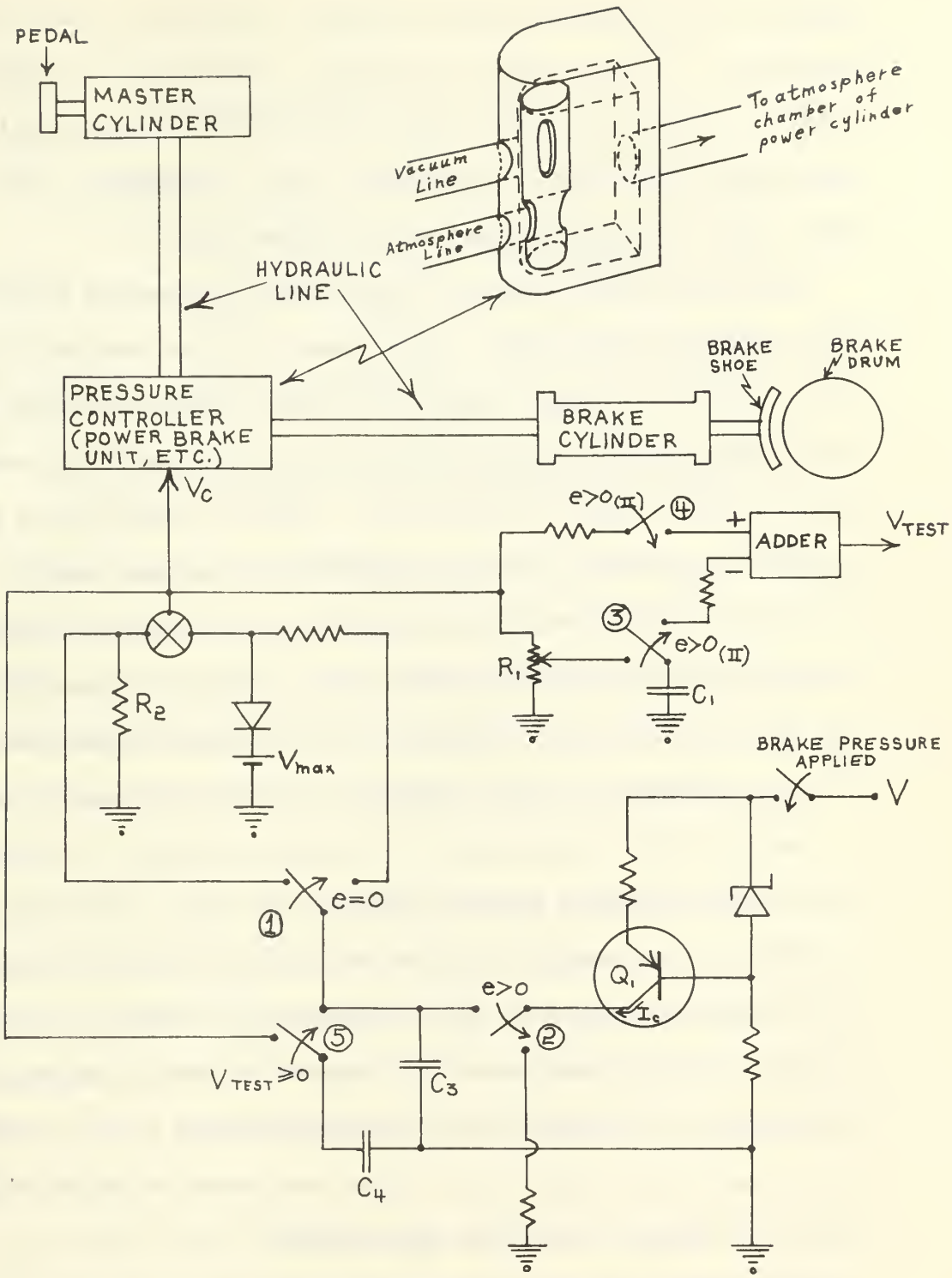


**Fig. 35. Proposed implementation of the triple ramp control.**

Capacitor $C_3$ discharges rapidly through resistor $R_2$ (a very small resistance). $V_c$ thus drops very rapidly, permitting the braking force to be decreased toward zero; this step is an exponential decay with a very small time constant, but it approximates the first upward ramp of $F_c$ (shown with a slope of $K_3$).

When the error is reduced to zero (skid eliminated) switches ① and ② throw once more. The voltage on $C_3$ then starts to climb with a slope of $K_4$, thus causing the braking force to increase once more. During this first part of the cycle a portion of $V_c$ is being monitored by $C_1$ (thru the tap on $R_1$). When the braking force has increased sufficiently to cause skidding to occur once again, switches ① and ② throw once more and $V_c$ drops rapidly, decreasing the brake force as before. Additionally, however, switches ③ and ④ are now thrown, and capacitor $C_1$ has a charge proportional to the force required to cause skidding (say .9 x $V_c$ to cause a skid).

When $V_c$ falls sufficiently to eliminate the skid, e = 0 again, and the ramp generator charges $C_3$ upward once again. When $V_c$ is just equal to the charge on $C_1$ (.9 x $V_c$ to cause a skid, for example) $V_{test}$ becomes greater than zero, and switch ⑤ throws as indicated. This puts a large capacitance ($C_4$) in parallel with $C_3$ and causes the ramp slope to change to a much shallower slope (i.e., to change from slope = $K_4$ to slope = $K_c$). $V_c$ is thus caused to approach the value that creates a skid much more slowly.

When (or if) a skid occurs once more, the entire process described above repeats itself.

A sketch of the force acting on the brake cylinder is shown in Fig. 36.

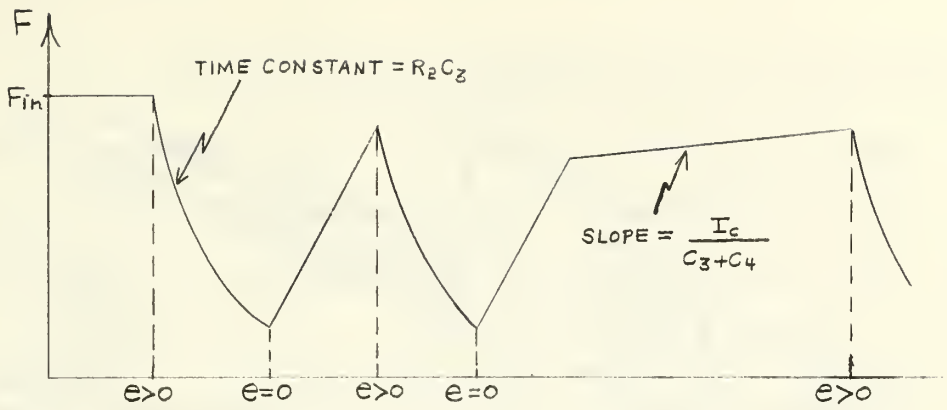


Fig. 36. Force acting on the brake cylinder during occurrence of one skid pair, if using Proposed Implementation.

Note also that the sensing of the first, third, etc., skids or second, fourth, etc., skids can be accomplished by an R - S flipflop connected to the output of a comparator which would be used to indicate the presence or absence of a skid. This was done on the analog computer simulation with very satisfactory results.

Figure 37 is a blow up of the pressure controller shown in the inset of Fig. 35. This is a standard form of control valve, and is not original with the Author.[1] A brief explanation of the workings of a standard power brake system, for which this particular form of implementation is ideally suited, is appropriate here.

In a power brake unit, when the brakes are applied, a valve to the atmosphere is opened on one side of a piston, and the other side is connected to a vacuum. The atmospheric pressure forces the piston closed, and causes pressure to be transmitted to the brake cylinder via a hydraulic line.

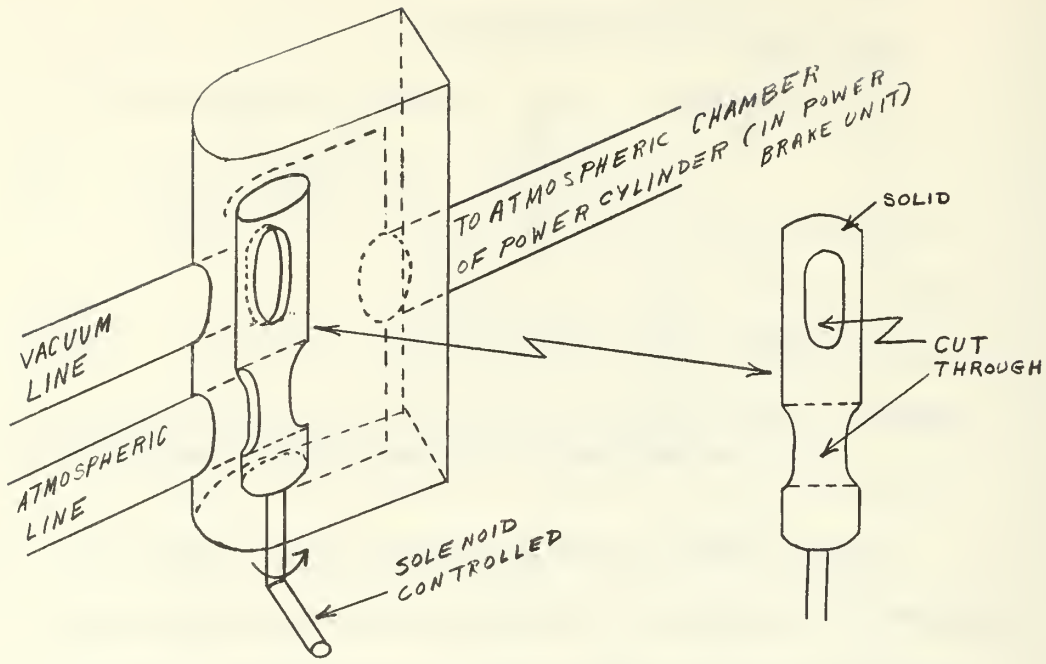


Fig. 37. Detail of pressure controller suitable for use with a power brake system.

The above controller will cause a disruption of the pressures on the power cylinder if the valve is rotated from the position shown. In the position shown, the vacuum line is blocked off thus permitting full atmospheric pressure to the piston; any other position of the valve would lessen the pressure on the piston, thus reducing the braking action.

## 9. CONCLUSIONS.

Of the three major types of controls simulated, the triple ramp control proved to be the only one lacking major defects, in that it reduced the degree of skid to a very low level while still providing a very short stop time. Nevertheless, the double ramp control was determined to provide a definite improvement over the completely uncontrolled situation, as did the bang-bang controls. However, for the double ramp control a slightly increased stopping time was the penalty paid for obtaining a lower degree of skid while stopping the vehicle. The bang-bang control with a dead zone proved unsuitable due to the presence of a slight degree of skid during the entire braking path of the vehicle. Additionally, the level to which the skid could be reduced would be severely limited by the response characteristics of the brake lines. The bang-bang control with a time delay, while still superior to the uncorrected situation, appeared to be considerably inferior to any other form of control simulated.

The triple ramp control, however, appears to provide very nearly optimum braking conditions in that the degree of skid and the skid time are both minimized, while still providing a considerably shorter stop time than would be obtained from any other form of control. A trade off between stop time and adaptability to improving road conditions is necessary though, and the proper balance between these two factors would be determined by both the type of vehicle involved and the anticipated road condition. However, greater emphasis should probably be placed on minimizing skid time and stop time by having a relatively low value for $K_c$.

The problem of possible oscillation introduced by the triple ramp control should never arise, since it is essentially a negative feedback system and should be inherently very stable.[6] Extremely unusual road conditions would probably be necessary for any oscillations to occur; however, an investigation of this subject has not been undertaken. This would possibly be a fruitful area for further study.

The response time required for the mechanical components of the proposed implementation of the triple ramp control (Fig. 35 and Fig. 37) would certainly be easily attainable. This may be seen from Fig. 25 (which is a "typical" response curve), where examination of the $F_c$ versus time curve indicates that the pressure controller would go through the high speed cycle at the rate of only about 4 c.p.s. This serves to give an order of magnitude approximation to the response characteristic necessary.

Throughout this entire thesis, $F_{in}$ has been assumed to be a constant, implying a panic stop situation with maximum force applied to the brake pedal. If, during the course of slowing the vehicle, the operator decreased the pressure applied to the brake pedal, no effect would be noticed in the operation of the automatic control, as long as the value of $F_{in}$ were still sufficiently large to cause a skid (if acting by itself). If, however, $F_{in}$ were decreased below the value needed to cause a skid (if acting alone), then the control would permit the net force F to rise to the new value of $F_{in}$ (either at the rate of $K_4$ or $K_c$, depending upon which part of the cycle was acting at the instant of decreasing the value of $F_{in}$) and this value of F would be retained until a skid once again occurred. If the

applied brake force $F_{in}$ were increased, the action of the triple ramp control would be unaffected, as the control would still continue to seek the optimum net force F.

A matter of possibly more concern is the characteristic of the linear accelerometer and of the integrator used to indicate the existence of a skid. The proper operation of this skid detecting scheme is basic to the operation of any skid correcting device proposed in this thesis. The mounting of the linear accelerometer would be very critical, and a position on the axle housing, in order to minimize "nose dive" effects, would be the most nearly ideal location. However, no serious theoretical limitations on the effectiveness of this form of skid detecting scheme present themselves, and this would appear to be the only practical means of detecting a skid prior to actual wheel lock up.

A final comment concerning the analog computer on which the brake system and all controls were simulated is appropriate at this time. The COMCOR Ci 5000 Analog Computer is in actuality a form of hybrid computer, in that extensive logic circuitry is available for use in conjunction with standard integrators and operational amplifiers. Simulation of this type of problem would be difficult if not impossible on a more conventional analog computer lacking the logic circuitry, high speed switches and overall versatility of this particular computer. A simulation of the type described would be possible on a digital computer utilizing one of the languages available for this purpose, such as DSL-360, etc. However, in order to obtain the extensive data needed to determine the performance characteristics of the various controls, large quantities

of very expensive digital computer time would be required. On the analog computer, however, almost two hundred different runs were made consecutively in a relatively short (and inexpensive) time period by merely varying potentiometer settings between runs. In this case, the accuracy of a digital computer was unnecessary, and the (hybrid) analog computer proved to be an exceedingly valuable design aid. This thesis thus illustrates graphically the continuing need for increasingly more sophisticated analog computers, such as the COMCOR Ci 5000.

# BIBLIOGRAPHY


1. White, A. J., Brake Dynamics. Research Center of Motor Vehicle Research of New Hampshire, Lee, New Hampshire, 1963.

2. Johnson, C. L., Analog Computer Techniques. McGraw-Hill Book Company, 1963.

3. COMCOR, Inc., Ci 5000 Operation and Programming Manual. COMCOR, Inc., Anaheim, California, 1967.

4. Chu, Y. H., Digital Computer Design Fundamentals. McGraw-Hill Book Company, 1962.

5. Phister, M., Logical Design of Digital Computers. John Wiley & Sons, Inc., 1962.

6. Clark, R. N., Introduction to Automatic Control Systems. John Wiley & Sons, Inc., 1962.

7. Halliday, D., and Resnick, R., Physics for Students of Science and Engineering. John Wiley & Sons, Inc., 1963.

8. The Encyclopedia Americana, Volume 12, FRICTION. Americana Corporation, 1959.

9. Wylie, C. R., Advanced Engineering Mathematics. McGraw-Hill Book Company, 1960.

10. Tomovic, R. and Karplus, W. J., High Speed Analog Computers. John Wiley & Sons, Inc., 1962.

Determination of the maximum possible deceleration of a vehicle.

The maximum deceleration possible for a vehicle is determined by the coefficient of friction between the tires and the road surface. Figure A1 represents an idealized vehicle traveling in the plus direction with a velocity $\dot{X}$, and a deceleration $\ddot{X}$, as indicated.

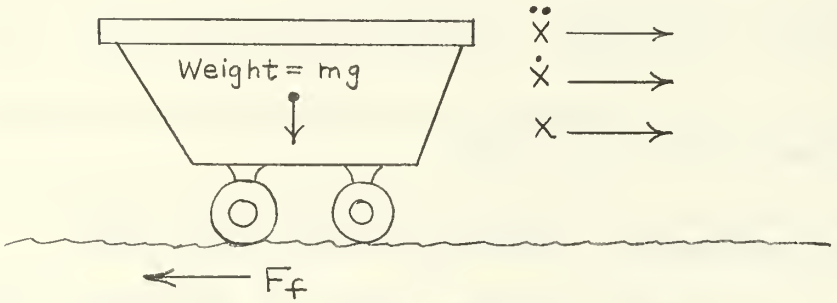


Fig. A1. Idealized vehicle.

In Figure A1, $F_f$ represents the force of friction acting on the vehicle, and is the only external force causing the vehicle to decelerate. The weight, mg, is the normal force acting on the ground, so the value of $F_f$ is given by

$$F_f = \mu mg \quad , \tag{A1}$$

where $\mu$ is the coefficient of friction between the wheel and the road surface. The coefficient of friction is a variable, which has its greatest value ($\mu_s$) just before a skid occurs, and then drops abruptly to a lower value $\mu_K$ when a skid begins.

Thus the maximum value of $F_f$ is

$$F_{f(max)} = \mu_s mg \ . \tag{A2}$$

Note that $\mu_K$ corresponds to the coefficient of kinetic friction, whereas $\mu_s$ corresponds to static friction.

Summing the forces in the X direction, we obtain

$$m\ddot{X} = - F_f \quad . \tag{A3}$$

Substituting Eq. (A2) in Eq. (A3) and solving for $\ddot{X}_{(max)}$, we obtain for the maximum possible deceleration

$$- \ddot{X}_{(max)} = \mu_s g \quad . \tag{A4}$$

## APPENDIX B

**Explanation of analog computer symbols used.**

The analog computer elements used in the simulations described in this thesis are indicated below.

**SYMBOL** | **DESCRIPTION**

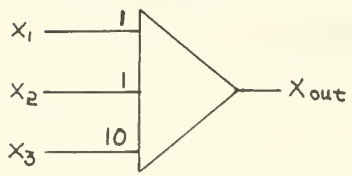


**Sign changing summer amplifier.**

$$X_{out} = -(X_1 + X_2 + 10X_3)$$

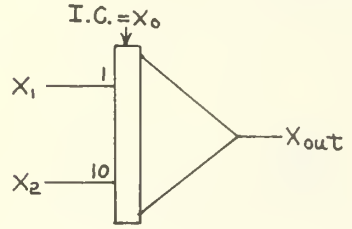


**Sign changing integrator.**

$$X_{out} = -\left[\int_{t_0}^{t_f} (X_1 + 10X_2)\, dt + X_0\right]$$

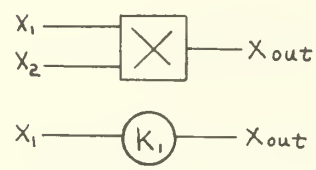


**Class III multiplier.**

$X_{out} = X_1 X_2$




**Potentiometer.**

$X_{out} = K_1 X_1$ , $K_1 \leq 1$

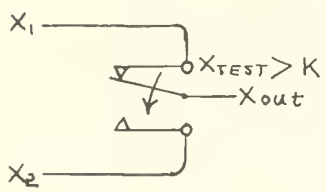


**Double pole, double throw relay.**

$X_{out} = X_1$ , for $X_{TEST} < K$

$X_{out} = X_2$ , for $X_{TEST} > K$


**High speed digital/analog switch.**

$X_{out} = 0$ , for $X_{TEST} < K$

$X_{out} = X_1$ , for $X_{TEST} > K$

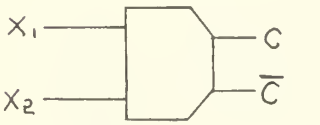


**Comparator.**

**C = logical 1 and $\bar{C}$ = logical 0, when $x_1 + x_2 > 0$.**

**C = logical 0 and $\bar{C}$ = logical 1, when $x_1 + x_2 < 0$.**

**Comparators are used to throw both the DPDT relays and the D/A switches.**

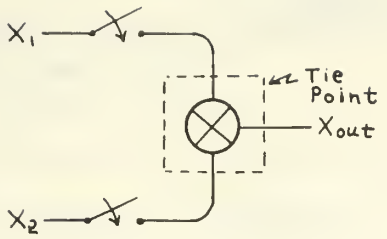


**Tie point.**

**Used in conjunction with two or more D/A switches which are thrown so that only one switch is ON at a time.**

$X_{out} = X_1$ or $X_2$

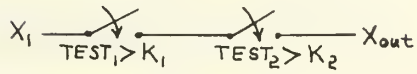


**Switching accomplished by NAND logic, utilising only one D/A switch.**

$X_{out} = X_1$, when

$(TEST_1 > K_1)$ and $(TEST_2 > K_2)$.

Also, $X_{out} = 0$, when

$(TEST_1 < K_1)$ or $(TEST_2 < K_2)$.

INITIAL DISTRIBUTION LIST

| | | No. Copies |
|---|---|---|
| 1. | Defense Documentation Center<br>Cameron Station<br>Alexandria, Virginia 22314 | 20 |
| 2. | Library<br>Naval Postgraduate School<br>Monterey, California 93940 | 2 |
| 3. | Professor Sydney R. Parker<br>Dept. of Electrical Engineering<br>Naval Postgraduate School<br>Monterey, California 93940 | 7 |
| 4. | Professor George A. Rahe<br>Dept. of Electrical Engineering<br>Naval Postgraduate School<br>Monterey, California 93940 | 1 |
| 5. | LT Douglas W. Harold, Jr.<br>8110 Richard Drive<br>Forestville, Maryland 20028 | 1 |

## DOCUMENT CONTROL DATA - R&D

*(Security classification of title, body of abstract and indexing annotation must be entered when the overall report is classified)*

1. ORIGINATING ACTIVITY *(Corporate author)*
Naval Postgraduate School
Monterey, California 93940

2a. REPORT SECURITY CLASSIFICATION
Unclassified

2b. GROUP

3. REPORT TITLE
Analysis and Design of a Suboptimal, Adaptive Automatic Braking System

4. DESCRIPTIVE NOTES *(Type of report and inclusive dates)*
Master of Science Thesis, June 1968

5. AUTHOR(S) *(Last name, first name, initial)*
HAROLD, Douglas W., Jr.

| 6. REPORT DATE | 7a. TOTAL NO. OF PAGES | 7b. NO. OF REFS |
|---|---|---|
| June 1968 | 92 | 10 |

8a. CONTRACT OR GRANT NO.

b. PROJECT NO.

c.

d.

9a. ORIGINATOR'S REPORT NUMBER(S)

9b. OTHER REPORT NO(S) *(Any other numbers that may be assigned this report)*

10. AVAILABILITY/LIMITATION NOTICES
This document is subject to special export controls and each transmittal to foreign government or foreign nationals may be made only with prior approval of the Naval Postgraduate School. Approved for public release 10/70

11. SUPPLEMENTARY NOTES

12. SPONSORING MILITARY ACTIVITY
Naval Postgraduate School
Monterey, California 93940

13. ABSTRACT

A mathematical model of a vehicle being brought to rest in such a manner as to cause a skid is devised and simulated on an analog computer. This model includes the effects of the brake line pressure upon the braking of the vehicle and also the effects of the coefficients of friction between the tire and road surface and between the brake shoe and brake drum. Several controls to correct for the occurrence of a skid are simulated on the analog computer and a detailed analysis of the braking system under the influence of each control is performed. Lastly, a scheme for implementing the control which minimizes the stop time and the degree of skid is presented.

DD FORM 1 JAN 64 1473

| 14 KEY WORDS | LINK A | | LINK B | | LINK C | |
|---|---|---|---|---|---|---|
| | ROLE | WT | ROLE | WT | ROLE | WT |